Geomorphology 452 (2024) 109096

Contents lists available at ScienceDirect

Geomorphology

journal homepage: www.journals.elsevier.com/geomorphology

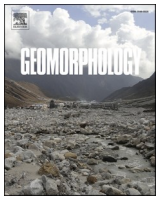

A Late Pleistocene coastal plain pertaining to MIS 5 in the Gulf of Cádiz (mouth of the Guadalquivir River, SW Iberia)

Antonio Rodríguez-Ramírez [a,b,*], Francisco Javier Gracia [c], Juan Antonio Morales [a,b], Diego García [d], Eduardo Mayoral [a,b]

[a] Departamento de Ciencias de la Tierra, Facultad de Ciencias Experimentales, Campus de el Carmen, Universidad de Huelva, Huelva, Spain
[b] CCTH - Centro de Investigación Científico Tecnológico, Universidad de Huelva, Huelva, Spain
[c] Departamento de Ciencias de la Tierra, Universidad de Cádiz, Cádiz, Spain
[d] Departamento de Humedales & Laboratorio de SIG y Teledetección, Estación Biológica de Doñana (CSIC), Sevilla, Spain

ARTICLE INFO

Keywords:
Late Pleistocene coastal plain
Littoral geomorphology
MIS 5
SW Spain

ABSTRACT

The geomorphological, sedimentological, topographical and chronological analysis of a large area located on the left bank of the Guadalquivir estuary (SW Iberian Peninsula), has enabled an extensive Late Pleistocene coastal plain to be defined, featuring a series of littoral strands. These rest uncomfortably on a rocky basal unit (*BU*) from the Lower Pleistocene, with an age of 1.1 Ma BP, showing shore platform morphology. The Late Pleistocene coastal plain presents a facies system where three stratigraphic units have been defined (*CPU 1*, *2* and *3*). All units indicate the progradation of a littoral barrier system towards the sea and correspond to highstand MIS 5e2. Above these is located a red sands unit (*RSU*), interpreted as alluvial deposits, and indicative of a gradual drop in sea level and a progressive continentalization of the area. This unit was affected by karst processes. According to the topographic elevation of these littoral strands, the relative tectonic stability of the area and the regional correlation, the elevation of the deposits, about 7–8 m above the current mean sea level, could be considered as a reasonable representation of the eustatic level during MIS 5e2. This data could be useful for comparison with other regional determinations of MIS 5 sea level in Western Europe, and for future predictions of relative sea level rise in the area.

1. Introduction

Coastal landforms and deposits are excellent geoarchives of geodynamic conditions in the past, since they usually provide magnificent information on climate, marine dynamics and tectonic processes during the Quaternary (Zazo et al., 2005; Stocchi et al., 2018). Preserved on a regional to global scale, coastal geomorphology often reflects regional patterns (Inman and Nordstrom, 1971). From Late Pleistocene to the present (the last 129,000 yrs., from the Marine Isotope Stage 5 onwards, NEEM, 2013), moderately rapidly oscillating sea levels favored the development of well-identified strandlines (Pedoja et al., 2014). However, a problem inherent with those deposits is that the intense dynamics associated with coastal environments often tend to erase or substantially erode them, especially when they are ancient. Moreover, in recent times the Holocene marine transgression could have buried or eroded previous geomorphological and stratigraphical evidence of many previous coastal environments (Fairbanks et al., 2005). In many cases the only remains lie below sea level, like the Pleistocene formations of the Dover Strait (García-Moreno et al., 2019).

This relative scarcity of outcrops of Pleistocene coastal deposits reduces the information needed for understanding in detail their original extension, and the palaeoenvironmental conditions responsible for their generation and development, including the relative sea level changes with which they were associated (Chappell et al., 1996; Siddall et al., 2008). There are various studies of the coastal environments prevailing in Western Europe during the Pleistocene highstands, particularly of those of a more recent origin, although the evidence is scarce, and the correlation between the preserved sites remains problematic (Whittington and Hall, 2002; Zazo et al., 2003; Benedetti et al., 2009; Rovere et al., 2016). This is a topic of particular significance today, as it could help to predict the development of current sea levels and the associated morphological consequences that could be expected to occur on the

* Corresponding author at: Departamento de Ciencias de la Tierra, Facultad de Ciencias Experimentales, Campus de el Carmen, Universidad de Huelva, Huelva, Spain.
E-mail address: arodri@uhu.es (A. Rodríguez-Ramírez).

https://doi.org/10.1016/j.geomorph.2024.109096
Received 21 October 2023; Received in revised form 5 February 2024; Accepted 6 February 2024
Available online 15 February 2024

coast.

Coastal records in the Gulf of Cádiz (SW Iberian Peninsula) have received considerable attention, especially those formed during the Holocene, because they are abundant and in general present a good state of preservation (Zazo et al., 1994, 2008; Lario et al., 1995; Goy et al., 1996; Rodríguez-Ramírez et al., 1996, 2015; Rodríguez-Ramírez and Yáñez, 2008; Morales, 1997; Gutiérrez-Mas et al., 1996; Borrego et al., 1999; Caporizzo et al., 2021). They are mainly concentrated on estuarine environments, associated with the mouths of the most important rivers draining the Southern and SW portion of the Iberian Peninsula (Borrego et al., 1999; Boski et al., 2008; Sampath et al., 2015, among others). The technique commonly used for their study consists of the sedimentological interpretation and dating of boreholes (Dabrio et al., 2000; Delgado et al., 2012; Lario et al., 2015). Of all the extensive estuaries in the Gulf of Cádiz, of the Guadalquivir River is the most important for its dimensions, variety of environments and records associated with its historical evolution, and its high ecological value (García-Novo and Marín Cabrera, 2006; Rodríguez-Ramírez et al., 2019).

By contrast, outcrops dating from the Pleistocene in the same area are scarce and less extensive (Zazo, 1980; Zazo et al., 2003; Aguirre, 1995; Hernández-Molina et al., 2002; Bardají et al., 2009; Gutiérrez-Mas and Mas, 2013; González-Acebrón et al., 2016), and have always been studied from a stratigraphic and sedimentological perspective. These outcrops correspond to levels of coarse-grained beaches with the morphology of marine terraces that appear on coastal cliffs and rock platforms in the intertidal zone, and which were often defined as erosional palaeoshorelines (Pedoja et al., 2014). The few existing outcrops and the inability to follow them inland have made impossible to draw any kind of conclusion with regard to their geomorphological and palaeodynamic configuration or their spatial extension.

These limitations can be overcome with high-resolution altimetry techniques, such as LiDAR (Light Detection and Ranging), which can identify subtle morphologies invisible to traditional methods (Cracknell, 1999). One of the most valuable features of LiDAR is the ability to quickly inspect large areas of land, since it allows multiple physiographic variables to be interrelated (Boak and Turner, 2005). This method has revealed the extraordinary extension of certain Pleistocene highstands in the Gulf of Cádiz, something that had not been possible to determine until now. The application of LiDAR enabled the visualization of the detailed topography of an extensive Quaternary coastal plain in a sector of the Gulf of Cádiz located on the left bank of the Guadalquivir estuarine channel. The geographical analysis and its relationship to other similar deposits in the region have allowed the outcrop to be contextualized in a very similar way to those found in other sedimentary coastal areas (Villwock, 1984; Otvos, 2005; Bateman et al., 2004; Zazo et al., 2013, among others).

The main objective of this work is to analyze the geomorphological and sedimentological features of the Quaternary coastal formations recognized within the study area of the Atlantic coast of SW Spain, and to establish them within a chronological framework. These features will allow the morphostratigraphy of the geological formations of this coastal sector of the SW Iberian Peninsula to be established, along with the implications for the local and regional geodynamic framework. All these units are compared to other outcrops of a similar nature and age located in the immediate environment so as to establish the sea level during this highstand period. Apart from the heritage value inherent to such geomorphological records, the information obtained from the study also allows the geomorphological consequences of the present sea level rise to be predicted along the coast of the Gulf of Cádiz, taking the previous interglacial period as a model.

2. Study area

The area of study is located in the Gulf of Cádiz, on the Atlantic coast of SW Spain, between coordinates 36°40′N-6°20′W and 36°47′N-6°28′W. The studied Pleistocene formations are located on the SW margin of the Guadalquivir Foreland Basin and to the west of the Betic Mountain Range (Fig. 1). These formations outcrop along the coast of the towns of Sanlúcar-de-Barrameda, Chipiona and Rota, where a rock platform and a coastal cliff 3–5 m in height leads to the exposure of a Quaternary stratigraphic sequence. Inland, these formations extend for about 4–5 km along an intensely agriculturally transformed coastal plain with gentle orography, which rises approximately 4 to 8 m above sea level. To the east, this coastal plain ends in some reliefs of gentle hills that rise to a height of 70 m, made up of Pliocene and Miocene formations of marls, clays and sands. These Neogene outcrops are part of the formations on the SE orogenic margin of the Guadalquivir Foreland Basin.

The study area is considered a tectonically active region (González-Castillo et al., 2015), located in the convergence zone of the European and African plates. There is a fault system that affects both the Mio-Pliocene formations and the Pleistocene units (Viguier, 1977; Roldán et al., 1988; Sanz de Galdeano and López Garrido, 1991) and determines the rectilinear stretches of the coast and most of this coastal region as far as the Strait of Gibraltar (Fig. 1). Dating of Pleistocene perched deposits in Gibraltar Rock provided maximum uplift rates of 0.33 ± 0.05 mm/yr for the 240–200 ka BP period, and a later decrease to 0.005 ± 0.01 mm/yr for the Late Pleistocene-Present period (Rodríguez-Vidal et al., 2004). North of Gibraltar, in the Bay of Cádiz, accumulated horizontal displacements recorded during the Quaternary can exceed 2 km, while vertical motion hardly reaches some tens of meters, indicating a prevalent transcurrent tectonic regime (Gracia et al., 2008). In the Guadalquivir estuary differential subsidence and sedimentary infilling was controlled by the Pleistocene activity associated with the fault system represented in Fig. 1 (Rodríguez-Ramírez et al., 2014). The fault families in the area are arranged in SW-NE and NW-SE directions, and have a main strike-slip component. They are related to the regional NW-SE to N-S compressive regime, with associated EW extension (Zazo et al., 1999; Silva et al., 2006; Gracia et al., 2008; Grützner et al., 2012; Martínez-Loriente et al., 2013; González-Castillo et al., 2015). No numeric data exists about the recent to present rate of vertical movements related to tectonic activity in the area. The strong subsidence recorded in the center of the Guadalquivir estuary for the 4000 to 2000 cal. yr BP period, and a later subsidence decrease which favored coastal progradation and relative sea-level stability, were processes interpreted by Rodríguez-Ramírez et al. (2014) as indirect consequences of the recent tectonic activity in the region.

Regarding the geodynamic conditions, the Guadalquivir River estuary borders the northern limit of the study area. This river is the most important fluvial network in SW Iberian Peninsula, with a mean discharge of 164 m^3/s, although during winter floods can occasionally exceed 5000 m^3/s and exceptionally 10,000 m^3/s (Vanney, 1970). Concerning marine dynamics, the mean tidal range in the area is 2 m with extreme spring tidal ranges of 3.86 m (Spanish Ministry of Fomento, 2005). Prevailing winds come from the SW and are especially significant during Atlantic storms, which occur during autumn-winter, generating a maximum significant wave heights of 4 m (Benavente et al., 2000). These storm waves intensely erode the coast, usually affecting coastal infrastructures. The littoral drift current depends on the orientation of the coast with respect to these wave trains: along the Chipiona-Sanlúcar de Barrameda stretch it is directed towards the NE, whereas along the Chipiona-Rota stretch it flows to the SSE.

3. Methodology

3.1. Geomorphology

Detailed field studies of the Pleistocene formations were carried out, complemented by a general geomorphological analysis from aerial images taken in 1956 (U.S. Army photogrammetric flight), allowing the natural configuration of the territory to be obtained before agricultural and urban uses transformed the lands in the subsequent decades. The

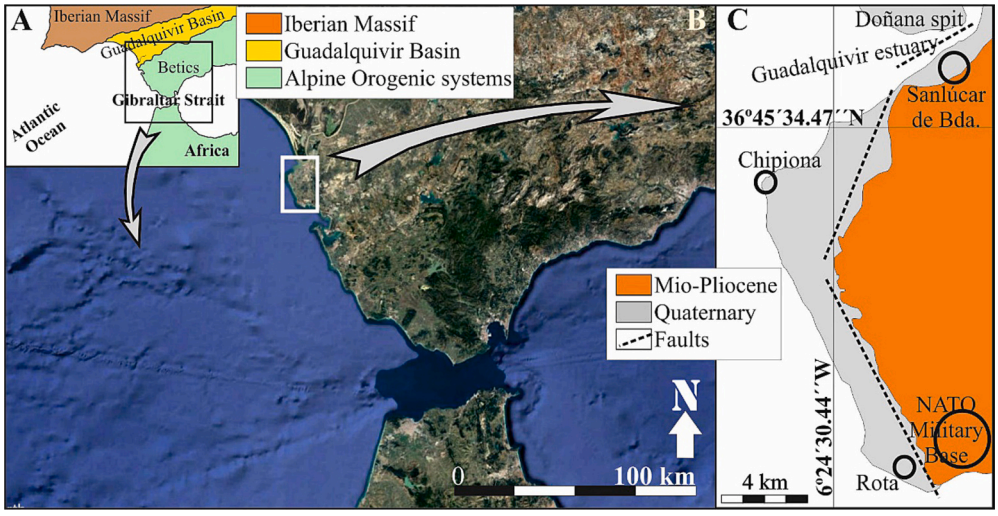

Fig. 1. A.- Regional geological setting, B.- Location of the study area in the SW of Spain, C.- Geological setting of the study area. Dashed lines indicate the main morphostructural lineations in the zone.

detailed topographic data was analyzed from a digital elevation model (LiDAR surveying) from 2020, of the Second Coverage of the Spanish National Orthophoto Program (PNOA), and processed by means of the software Global Mapper v. 23. The topographic analysis was performed on a DTM (Digital Terrain Model) generated from the raw.laz files (3D point cloud). The 3D point cloud was filtered (bounce, height above ground, color) in order to keep only ground points, with which the DTM was finally created at 2 m spatial resolution. The referenced topographic altitude and mean sea level were adjusted to the mean sea level for the Gulf of Cádiz, located about 30 cm above the national topographic zero (Spanish Ministry of Public Works, 2005).

3.2. Lithology and morphostratigraphy

Along the existing coastal cliff in the study area, a series of stratigraphic sections were logged to establish a detailed sedimentological configuration and describe the facies of the Pleistocene formations. The lithostratigraphic study aims to characterize the sedimentary facies, the geometry of sedimentary bodies and surficial morphology, as well as the relationships between them. Grain-size analyses were performed using conventional sieving for fractions >2 mm and a Malvern Mastersizes 2000 laser diffraction particle analyzer for smaller particle sizes (between 2 mm and 2 μm). Shepard's sediment classification (Shepard, 1954) was applied to grain-size results in order to describe sediment texture, including gravel, sand, silt and clay fractions.

3.3. Dating

To determine the age of the sedimentary formations, 3 samples were taken and dated by $^{87}Sr/^{86}Sr$, and another 3 by OSL (Optically Stimulated Luminescence). The altitude of the samples locations was taken with a Garmin GPSMAP 65. Table 1 includes data related to the dating of the 6 samples. To establish the $^{87}Sr/^{86}Sr$ isotopic ratios, samples were taken from well-preserved shells, located in specific positions of the stratigraphic sections. Sr isotopic ratios were analyzed on a TIMS-Phoenix Mass Spectrometer from the UCM Laboratory of Isotopic Geochronology and Geochemistry (Universidad Complutense de Madrid). These isotopic ratios were corrected for possible interference from ^{87}Rb and normalized to the value of $^{87}Sr/^{86}Sr = 0.1194$, to correct the possible isotopic fractionation effect during the measurement. Samples analyzed by $^{87}Sr/^{86}Sr$ method were referred to NBS-987 standard (0.710247). Geological ages were determined based on the look-up table of Farrell et al. (1995).

The sedimentary units selected for dating using OSL were collected using opaque tubes 60 mm in diameter with a wall of 3 mm, avoiding the exposure of the inner sediment to daylight. Measurements were carried out using standard procedures on quartz grains 180–250 μm in size, extracted from each sample under controlled light conditions (Wintle, 1997). The measurements were performed using automated Risø TL/OSL DA-20 luminescence readers, equipped with $^{90}Sr/^{90}Y$ beta sources providing doses rates of ~0.10 Gy/s at the sample position. Quartz multi-grain aliquots were measured following the Single-Aliquot Regenerative-Dose (SAR) protocol (Murray and Wintle, 2000, 2003) to obtain representative dose distributions. The derived dose populations were reduced by removing the outliers, identified as those out of 1.5 times the interquartile range. The equivalent dose (De) was estimated applying the Central Age Model (CAM, Galbraith et al., 1999) on the reduced population. Environmental dose rates, DR, were calculated as a

Table 1
Chronology of the dated samples. Altitude above mean sea level in the Gulf of Cádiz.

Sample	Altitude	Method.	Lab. code	NBS-987	+Std Err*10^{-06}	Type of sample	Age(Ka)
D1	3.6 m	$^{87}Sr/^{86}Sr$	Cádiz M_1	0.709160	2	Shell (Chlamys)	≈150
D2	−0.1 m	$^{87}Sr/^{86}Sr$	Cádiz M_2	0.709113	2	Shell (Pecten)	≈1100
D3	−0.2 m	$^{87}Sr/^{86}Sr$	Cádiz P3	0.709116	2	Shell (Oyster)	≈1100

Sample	Altitude	Method.	Lab. code	Dose rate (Gy/Ka)	Equivalent dose (Gy)	Type of sample	Age (Ka)
D4	6 m	OSL	LM20139-04	1.54 ± 0.07	152.8 ± 4.5	sand	99.1 ± 5.3
D5	4.3 m	OSL	LM20139-02	1.03 ± 0.05	107.46 ± 4.45	sand	104.9 ± 6.8
D6	4.5 m	OSL	LM20139-01	1.25 ± 0.06	173.9 ± 6.5	sand	139.3 ± 8.8

contribution of beta, gamma and cosmic radiations. They were derived from radionuclide activity concentration determined by high-resolution gamma spectrometry (HPGe), measured at the Radioisotopes Unit (RDI) at the University of Seville.

The doses received by the samples due to the radionuclide concentration in the sample matrix were calculated using appropriate conversion factors (Guerin et al., 2011). A linear accumulation of deposits was assumed in order to calculate the contribution of cosmic radiation according to the burial depth, latitude, altitude and average over-burden density (Prescott and Hutton, 1994). The total dose rates were corrected according to attenuation caused by moisture and grain size. A 5 % error was added to the estimated water content used for the correction. Environmental dose rates to an infinite matrix value were calculated using the Dose Rate & Age Calculator (DRAC, Durcan et al., 2015).

4. Results

4.1. Geomorphology

From a geomorphological point of view, an extensive coastal plain spreads across the study area at an altitude between 5 and 9 m above the mean sea level (Figs. 2 and 3). This plain extends about 3–5 km inland, to border a relief of gentle hills constituted by marls, clays and sand formations of Mio-Pliocene age. The boundary between the coastal plain

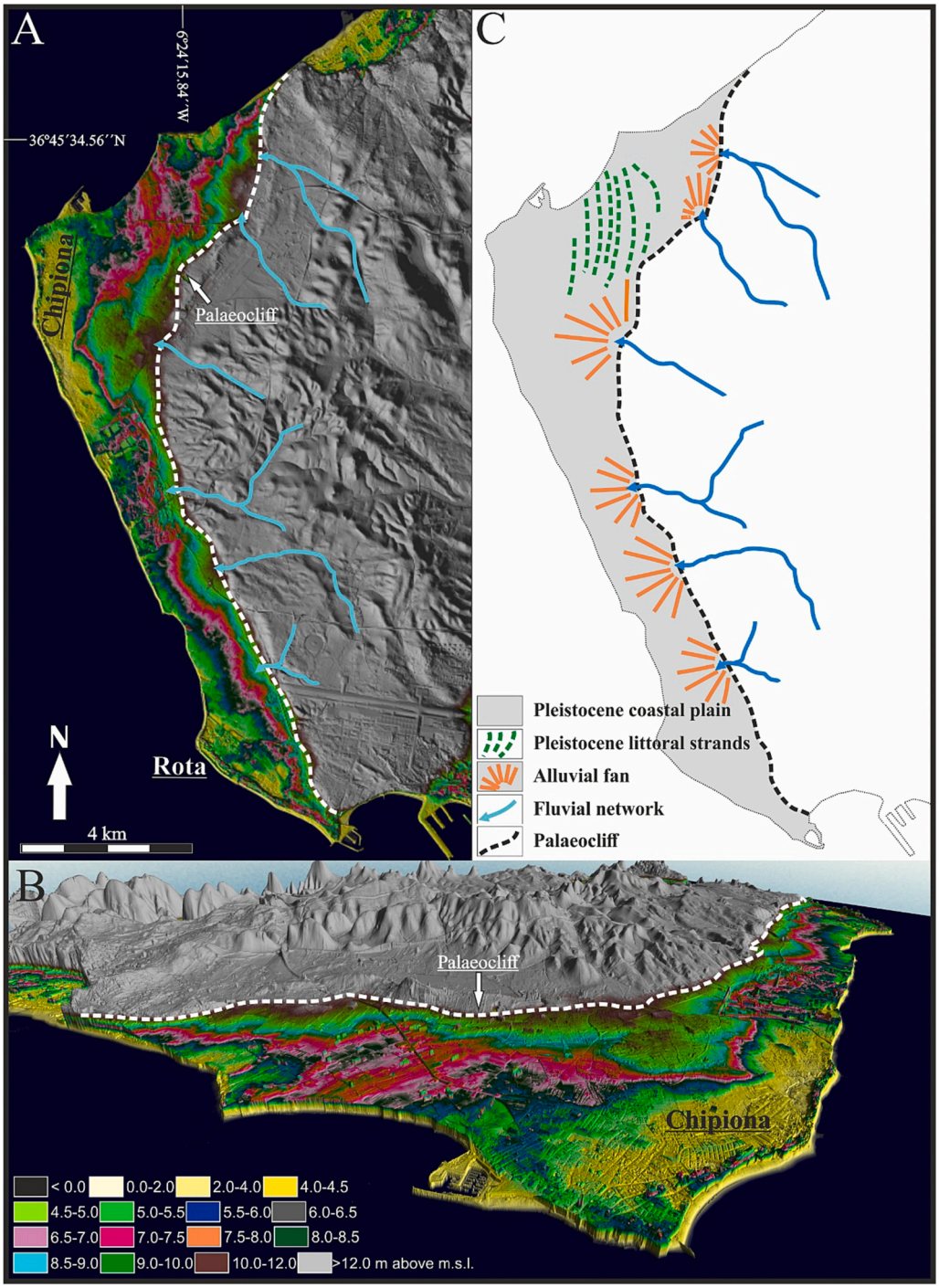

Fig. 2. A and B.- 3D LiDAR model. C.- Geomorphological scheme. The color legend corresponds to the elevation intervals above mean sea level in meters.

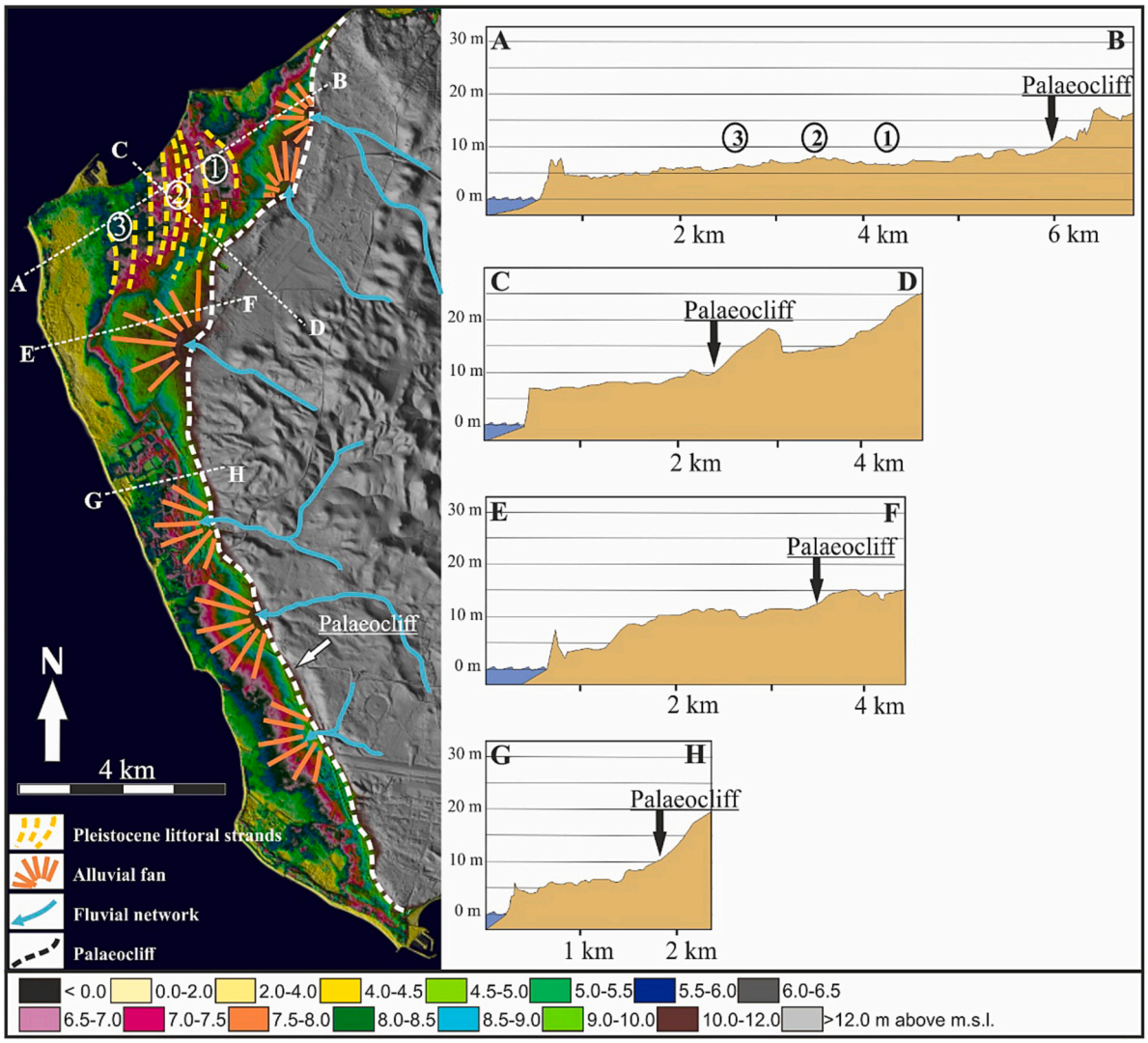

Fig. 3. Topographic profiles in the study area.

and these hills is marked by a conspicuous escarpment interpreted as a palaeocliff. This escarpment can be divided in two stretches; the one between Chipiona and Sanlúcar de Barrameda, with a broad direction N20°-30°E, and the one between Chipiona and Rota, with a marked rectilinear outline following the direction N155°-160°E. These escarpments are conditioned by two fault families acting in these directions (Fig. 1). Their continuity is interrupted by the incision of the fluvial network and a series of alluvial fans partially covering the coastal plain.

On the coastal plain, a series of very subtle parallel longitudinal low reliefs can be distinguished, detected only by the altimetric precision supplied by the LiDAR flight. These are aligned in an approximate N-S direction and slightly curved towards the west (Fig. 2). The most visible ones are arranged alternately in up to 5 ridges and swales as littoral strands. The most prominent ridge is located in the central area and presents an elevation of about 8 m (number 2 in section A-B of Fig. 3). Laterally, the rest of the ridges present a decreasing height until reaching about 6 m (nos. 1 and 3 in section A-B of Fig. 3). The unevenness between ridges and swales is decimetric, between 0.5 and 1 m. These coastal ridges and swales all seem to converge to the south, and finally attach to the escarpment that limits the coastal plain to the east (Figs. 2 and 3).

The western limit of the coastal plain with the sea is a continuous low cliff (2–5 m), where Holocene coastal formations (dunes, beaches, lagoons) develop in some sectors. From here, a conspicuous rock platform extends into the intertidal zone. These formations act as a substratum upon which the above-cited formations are arranged on the coastal plain. The rock platform is affected by a system of joints with a direction N 145°-150° E, similar to the escarpment main strike and parallel to the current rectilinear coastline between Chipiona and Rota. (Fig. 1).

4.2. Sedimentary facies of the Pleistocene coastal plain

Two sets of facies have been distinguished according to where they were observed. The first set, named as "Basal unit", was observed on the shore platform, whereas the second was identified in vertical outcrops in the cliffs (Coastal Plain units) (Fig. 4).

4.2.1. Facies observed on the shore platform (Basal units(BU))

These are located in the intertidal zone with a shore platform morphology (Figs. 5 and 6). They present several facies, all of them strongly cemented by carbonates.

4.2.1.1. Fine sandstones (Sh). These consist of tabular decimetric sandy layers mainly composed of fine and medium-grained sandstones. The grains are constituted mainly by well-rounded quartz, with a variable percentage of bioclastic shell fragments. The thickness varies between 10 and 25 cm. The stratification surfaces are commonly planar and depositional, and the internal ordering varies between be parallel

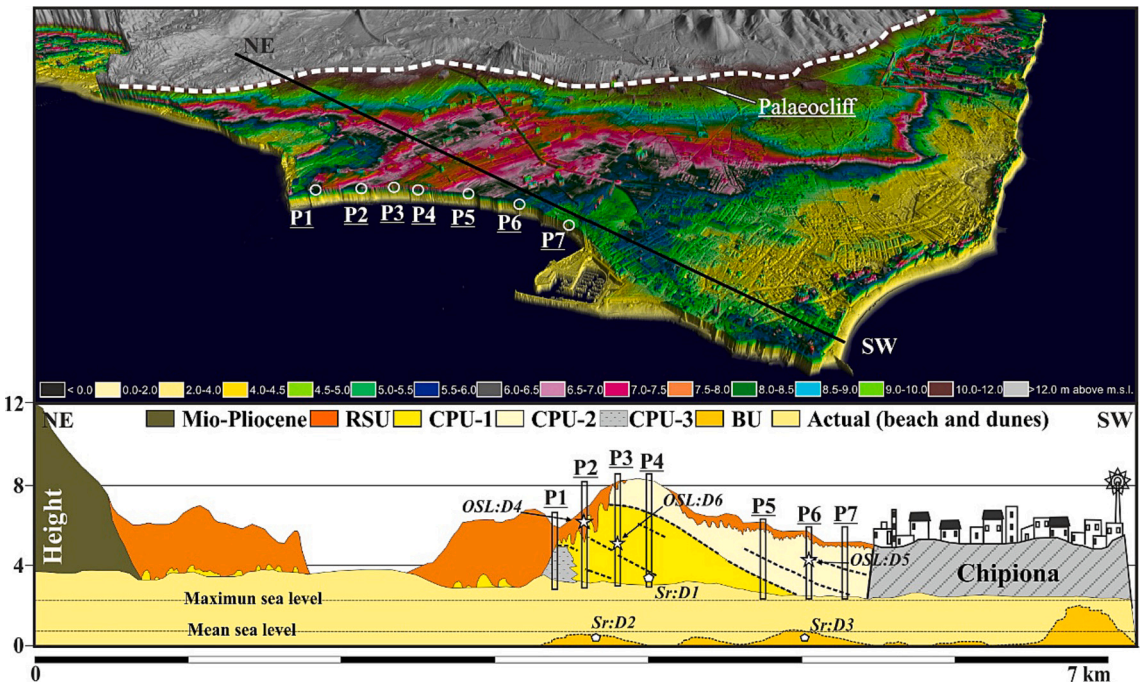

Fig. 4. NE-SW section of the coastal platform showing the profiles (P1 to P7) and arrangement of the units studied. Stratigraphic units: BU.- Basal units, CPU-1.- Coastal plain units 1, CPU-2.- Coastal plain units 2, CPU-3.- Coastal plain units 3, RSU. - Red sands unit.

Fig. 5. Left: A close view of the shore platform south of Chipiona city. Right: Extension of the shore platform in the study zone.

lamination or planar cross-bedding.

4.2.1.2. Very coarse sandstones (Sp). Some decimetric levels of very coarse bioclastic sandstones with abundant pebbles alternate with the facies described above. The base of these levels may be depositional or slightly erosive, and the typical internal ordering is planar or curved-base cross-bedding. The coarsest clasts (1–3 cm) are composed of quartz and quartzite and present a well-rounded surface. The thickness of these levels oscillates between a few decimeters and one meter.

4.2.1.3. Conglomerates (Gp). Metric conglomerate levels have also been observed. The base of each stratum presents an erosive surface, whereas the internal ordering presents landward-inclined planar crossbedding. The most abundant clast types include spheroidal quartz and quartzite pebbles (average diameter 2–3 cm). There are also present bioclastic clasts, mainly composed of fragments or entire valves of *Crassostrea*, *Glycimeris* and *Pecten*. Its thickness is usually several decimeters and only occasionally reaches about one meter. These conglomerate strata give rise to the more prominent reliefs on the shore platform (about 1–1.5 m high).

4.2.2. Facies observed in the cliff outcrops (Coastal plain units)

The main facies distinguished in the cliff outcrops are represented in Fig. 7.

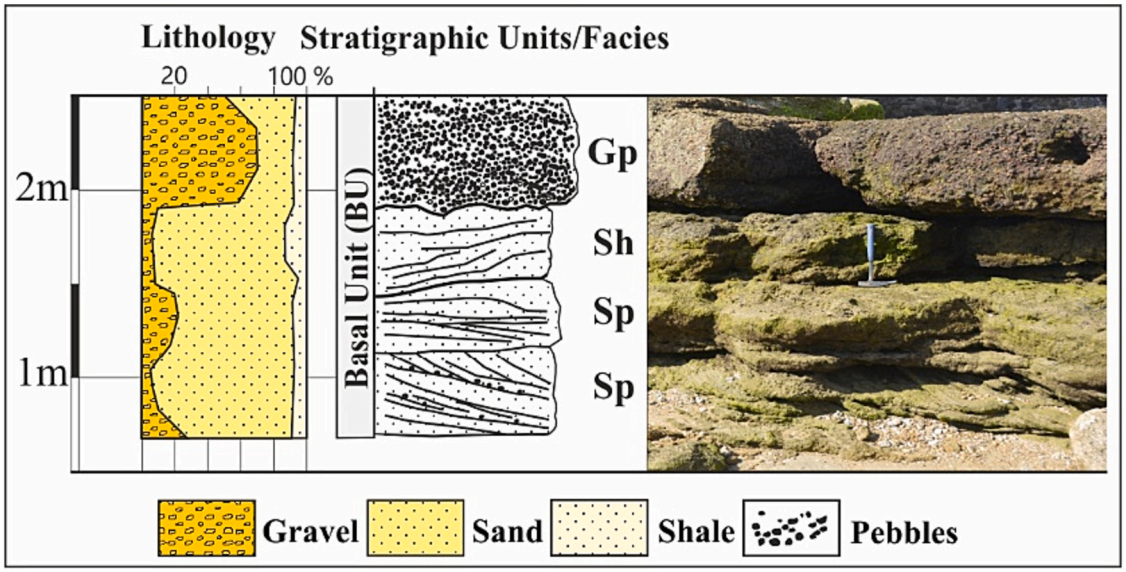

Fig. 6. Sequence of facies observed on the shore platform. Altitude above mean sea level in the Gulf of Cádiz.

4.2.2.1. Bioturbated silty sand facies (SFb). These are highly bioturbated grey-yellowish silty sands in which bioturbation has erased any previous sedimentary structure (Figs. 7, 8, 9 and 10). Most of the bioturbation observed corresponds to the activity of roots, although there are also vertical structures cemented by calcite, which correspond to burrowing, probably by crustaceans (*Ophiomorpha* ichnosp. indet.). These bioturbations form carbonate-cemented concretions.

4.2.2.2. Laminated silty sand facies (SFl). These are also constituted by grey-yellowish silty sand, although displaying a lower degree of bioturbation (Figs. 7, 8, 9 and 10). In this case, the lower intensity reveals an internal structure consisting of parallel horizontal or low-angle lamination. Both the top and the and bottom of these facies are typically erosive in nature. The lateral extension is metric, appearing as lenses into the bioturbated facies. The coarsest levels appear to be cemented by carbonates, in many cases highlighting the lamination.

4.2.2.3. Crossbedded sand facies (St). These are medium-to-coarse sands composed of mixed quartzitic and carbonated grains of bioclastic origin. In addition to isolated quartzite and carbonate clasts with a length of >2 mm, they also present loose or fragmented shells of ostreids and pectinids. The most notable feature is the appearance of sets of planar and curved base crossbedding, mostly with a north-northeast inclination (Figs. 7, 8, 9 and 10), sometimes separated by sets of parallel sheets slightly inclined towards the south. The contact with the overlying facies is irregular, but of a depositional nature.

4.2.2.4. Conglomerate facies (G). These are mostly cemented gravels made up of quartz, quartzite and carbonate pebbles, quartzite sandstone fragments, and loose shells of molluscs (Figs. 7, 8, 9 and 10). The clasts are always very well-rounded, with a diameter ranging between 20 and 50 mm. The thickness of the conglomerate levels ranges between 20 and 50 cm. The lower contact of these levels is always erosive and irregular, with positive grain-size classification. Some levels, especially those interspersed in the facies *St*, present large flattened pebbles of a carbonate nature (8–15 cm), which, to the NE, are usually imbricated.

4.2.2.5. Clay facies (Fb). These are greenish grey clays with horizontal lamination and numerous bioturbations from roots and crab cavities. The sandy interbedded laminations are not thick (1–5 cm), and the presence of molluscs (mainly ostreids and pectinids) can be observed, with obvious signs of transport (Fig. 7 and 8).

4.2.2.6. Red silty sand facies (SFm). These are red silty sands with scattered highly rounded clasts of quartzite. Intercalated clayey levels appear. No internal structure is evident, highlighting its massive nature, although some horizontal levels and lenses with a greater abundance of clasts can be observed (Figs. 7, 8, 9 and 10).

4.3. Stratigraphy and chronology

The base of the stratigraphic succession is constituted by the units described in the shore platform. The facies appear in cyclic sequences with rhythmic intervals of alternating fine sandstones (*Sh*) and very coarse sandstones (*Sp*). Conglomerate facies with an erosive base (*Gp*) occasionally appear intercalated between the rhythms (Fig. 6). The total sequence is separated from the upper unit, observed in the outcrops of the cliffs, by a scarcely visible unconformity.

Seven stratigraphic sections were studied in the outcrops of the coastal plain to establish the sedimentary sequences of the facies described above (Figs. 8 to 10). The facies in these sections are superimposed as fining-upwards sequences. Each begins with conglomerate facies (*G*) and ends with parallel laminated silty sands (*SFl*), or root-bioturbated silty sands (*SFb*) (Figs. 8 and 9). In some of the sequences, cross-bedded sands (*St*) occasionally appear in the conglomerate facies (Fig. 9, profile 4).

In the first three stratigraphic sections (P1 to P3) (Figs. 8 and 9), the facies *SFb* and *SFl* dominate the sequences, whereas in the sections P4 to P7 (Figs. 9 and 10), the facies *St* and *G* are more evident. Top terms of the succession were erosively dismantled. The correlation of sections P1, P2 and P3 allows us to infer how the facies developed vertically and laterally along the sedimentary bodies.

At the top of all sections, there is a body of red silty sand facies (*SFm*), separated from the sequences described above by an erosive unconformity, extensively altered by the karstification processes that affect the sedimentary sequence of the coastal plain. These sequences of red silty sand facies (*SFm*) are slightly inclined to the southeast on the horizontal strata of the shore platform.

Six samples were taken and chronologically dated (Table 1). Two of these samples were obtained from the sequences on the shore platform (D2 and D3), and four from the sequences in the cliff (D1 and D4 to D6).

A division in stratigraphic units was applied according to lithological and chronological criteria (Figs. 4, 6, 8, 9 and 10). The resulting units are as follows:

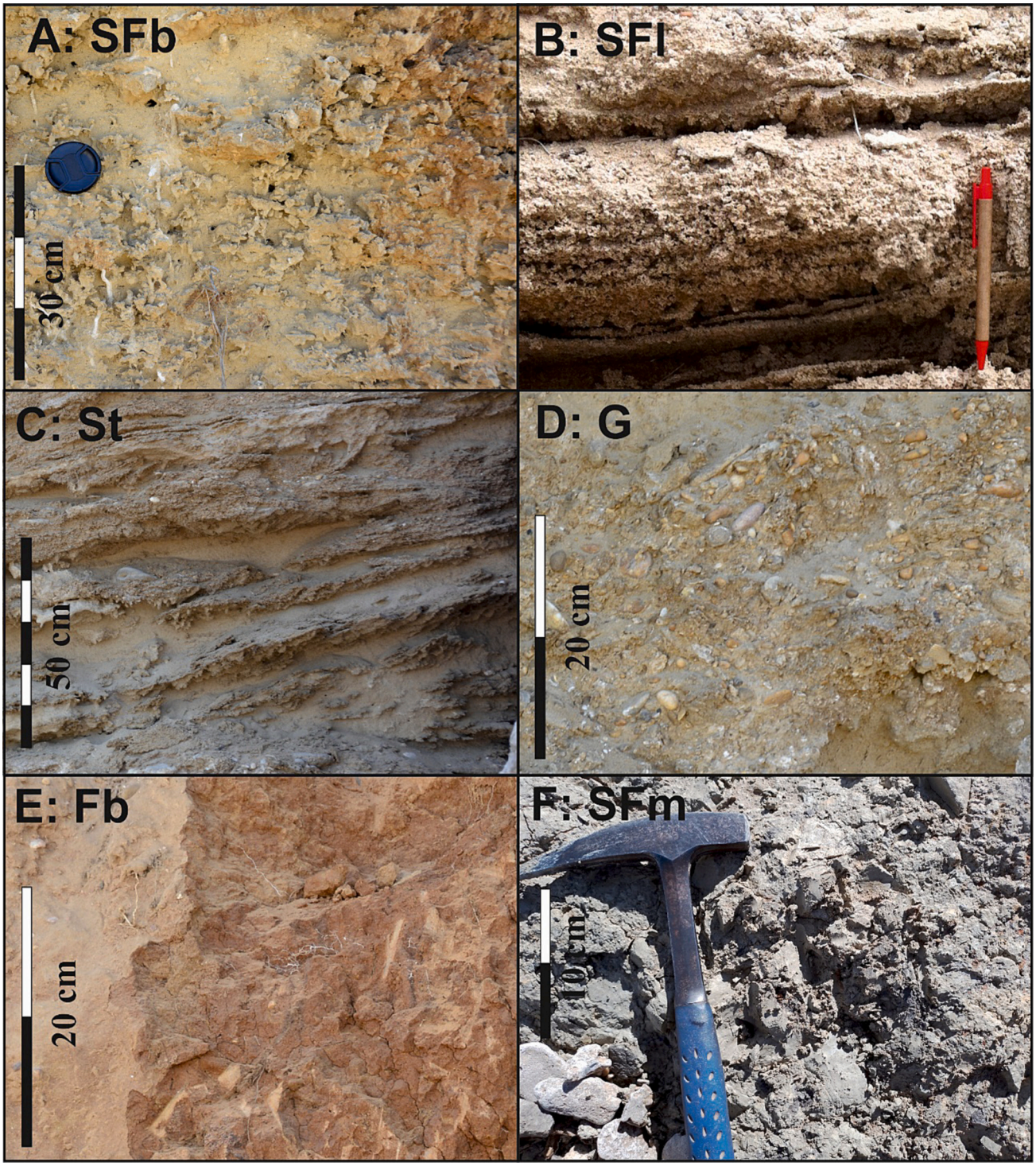

Fig. 7. Main facies distinguished in the cliff outcrops. SFb.- Bioturbated silty sand facies, SFl.- Laminated silty sand facies, St.- Crossbedded sand facies, G.- Conglomerate facies, Fb.- Clay facies, SFm.- Red silty sand facies.

4.3.1. Basal unit (BU)

This corresponds to the facies and sequences described in the shore platform, constituting the substrate or basement of the coastal plain units. The rock bodies are arranged horizontally or subhorizontally. In some sectors, they present a network of subparallel joints in the direction N135-155E. The dated samples give ages of about 1.1 Ma BP (Table 1).

4.3.2. Coastal plain units (CPU)

The main part of these units is constituted by the facies described above (*SFb, SFl, St* and *G*). These fining-upwards sequences overlap each other stratigraphically throughout the sedimentary succession, between successive erosive interruptions. Different superimposed sequences are slightly inclined towards the SW, offlapping above the basal unit. From a chronological point of view, two units can be distinguished. The lower unit (*CPU-1*) consists of three superimposed fining-upwards sequences separated by conglomerate levels with erosive bases (*St*). The upper unit

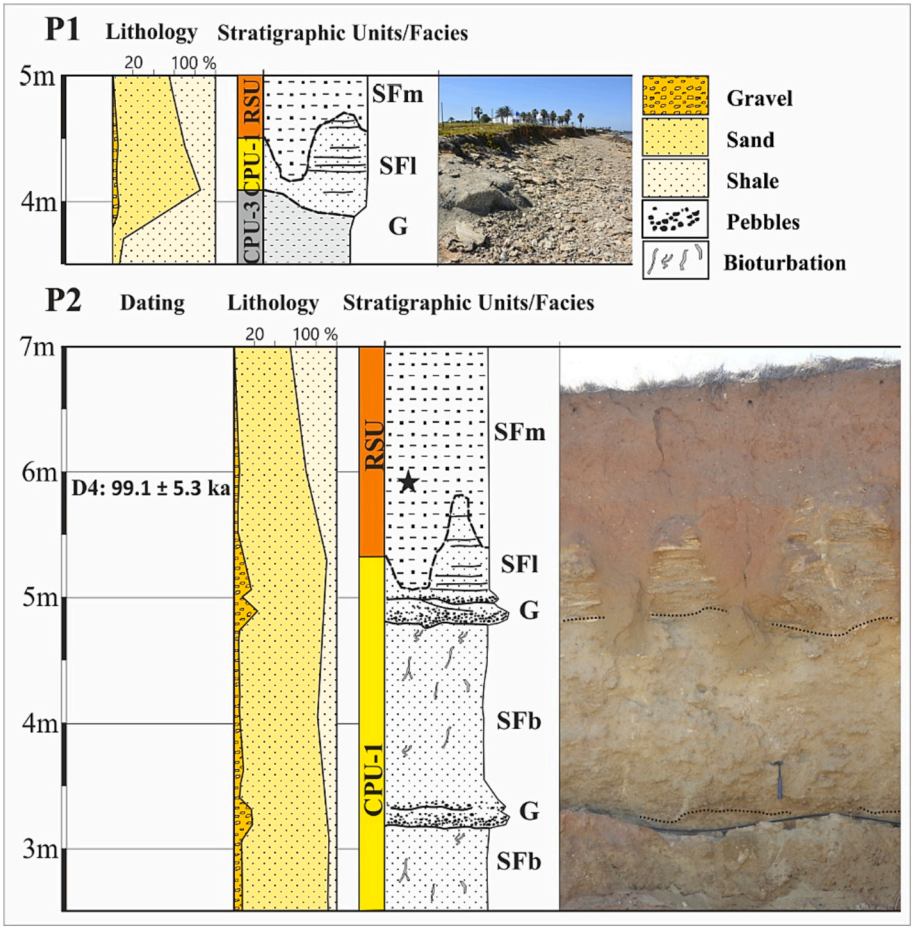

Fig. 8. Stratigraphic sections 1 and 2. Altitude above mean sea level in the Gulf of Cádiz.

(*CPU-2*) sits erosively on the lower unit in an offlap arrangement. This unit is constituted by two new sequences separated by conglomeratic levels. On the surface, these sequences constitute the littoral strands that extend over the whole coastal plain (Fig. 2).

The age of CPU-1 is in the range 139–150 ky BP (samples D1 and D6), corresponding to the end of MIS 6 and the beginning of MIS 5e2. CPU-2 is ca. 104 ky BP (sample D5), corresponding to the highstand of MIS 5c.

A third unit (*CPU-3*) outcrops to the northeast of the two first units of the coastal plain, at the foot of a cliff, and heavily eroded by marine dynamics. This unit is constituted only by dense greenish-grey clay facies (*Fb*). To the southwest, this unit interdigitates with the sandy facies of CPU-1. Consequently, a similar chronology can be deduced for both units.

4.3.3. *Red sands unit (RSU)*

All the units described above are affected by a palaeokarst in the upper part of the outcrop, giving rise to an unconformity with the overlying unit. The karstification surface is associated with a discontinuous, centimetres (1–3 cm) thick level of laminar type calcrete. The unit consists solely of red silty sand facies (*SFm*), which cover many of the different units constituting the coastal plain. The thickness reaches about 4–5 m in the leeward sector of the littoral strands. A sample of this unit was dated (D4), giving an age of 99.1 ky BP (MIS 5b).

5. Discussion

5.1. *Facies and morphostratigraphic interpretations of the Pleistocene coastal deposits*

Each facies can be interpreted in terms of its sedimentary environment. Thus, the rounded clasts of the Gp facies are characteristic of a constant reworking of the sedimentary material. Based on the lithology of the clasts, this type of facies is usually associated with fluvial sequences (Schumm, 1985; Miall, 1996). However, the presence of marine shell bioclasts between the siliciclastic clasts suggests a genesis in a coastal/marine environment. Since these facies appear interspersed with sandy facies, many of these levels could be interpreted as seasonal tempestites on a mixed sand and gravel beach similar to those described by Mason and Coates (2001), Horn and Walton (2007), and Roberts et al. (2013). Landward-dipped crossbedding in some of the gravel levels could also be interpreted as a product of pebble bars adjoining a high-slope reflective beach (Kirk, 1980).

The source of pebbles in all these facies seems to be related to previous fluvial deposits from the Guadalquivir River. Several remnants of ancient fluvial terraces located around the present sea level were identified and interpreted by Gracia et al. (2010) as linked to past courses of the Guadalquivir River during lowstand episodes in the Pleistocene. The prevailing littoral drift at that time, supposedly similar to the present and directed to the SE, would have produced the bending of the river to its left, protected from the sea by a confining sand barrier, as occurred during the Holocene and at present in all rivers emptying into the Gulf of Cádiz. The fluvial deposits consist of rounded pebbles whose composition indicates an origin from the Guadalquivir River basin (Palaeozoic

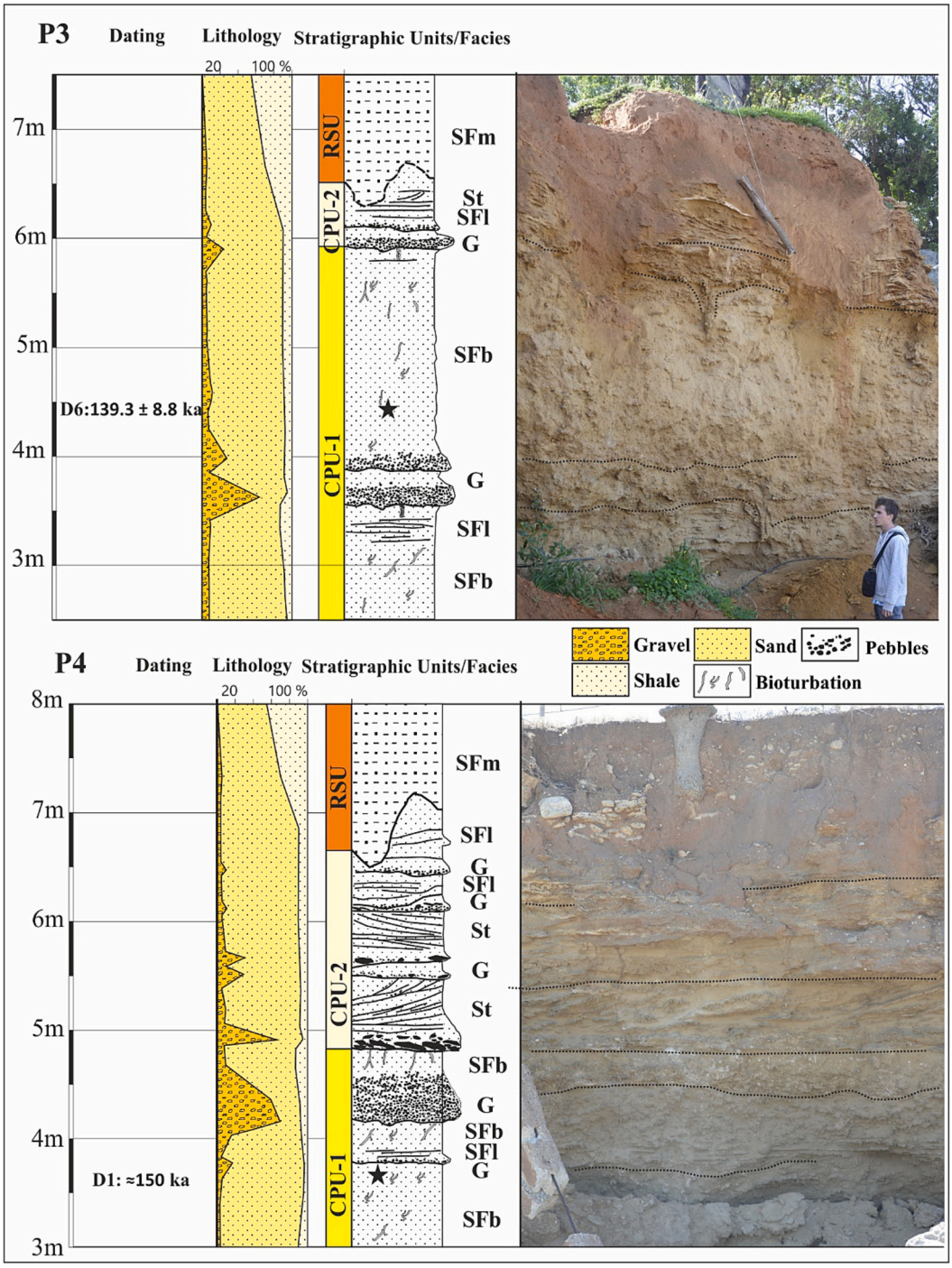

Fig. 9. Stratigraphic sections 3 and 4. Altitude above mean sea level in the Gulf of Cádiz.

quartzites, exclusively outcropping in the middle-high sections of the Guadalquivir basin). The track of such fluvial quartzite deposits can be followed along the coast to the SE as far as the nearby Bay of Cádiz, some 20 km away from the present mouth of the Guadalquivir (Gracia et al., 2010). These deposits would have supplied pebbles to the various coastal units, from the Basal Unit (*BU*) to the newer ones (*CPU-1* and *2*), including other Late Pleistocene deposits along this coast (Zazo et al., 1985; González-Acebrón et al., 2016; Achab et al., 2017).

A similar interpretation can be made with respect to the *St* facies (sands with scattered pebbles) of the Chipiona deposits: the superposition of landward-dipped crossbedding sets can also be assimilated with the attachment of bars in a beach, although in this case with a somewhat thinner grain-size, and transported by waves with lesser energy. Similar facies have been described in several places (e.g. Davidson-Arnott and Greenwood, 1974; Clifton, 1976, 2006; Tamura, 2012). The finer facies (*SFl* and *SFb*) correspond to less energetic environments. The laminated facies (*SFl*) could correspond to dissipative beach environments (Clifton, 1969), like many present beaches along this coast (Domínguez et al., 2005). The dominance of roots in SFb facies suggests their development in supratidal/aeolian backshore environments (Dashtgard and Gingras, 2005).

Each complete sequence is representative of a regression process, from a pebble beach foreshore (facies *G*), to a foreshore with bar attachment (facies *St*), followed by a plane dissipative beach (facies *SFl*),

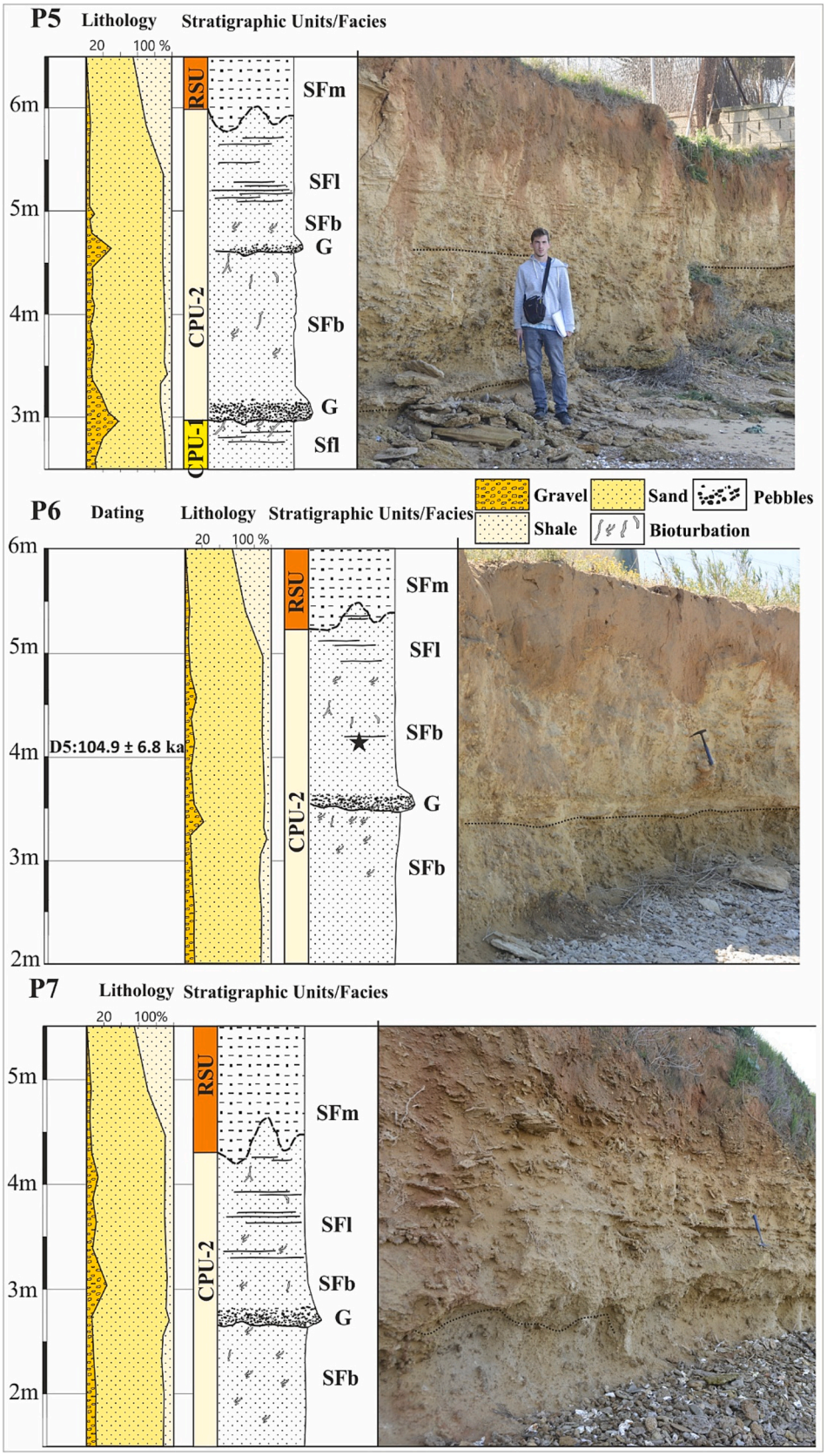

Fig. 10. Stratigraphic sections 5, 6 and 7. Altitude above mean sea level in the Gulf of Cádiz.

and finally ending with a backshore (Facies *SFb*). The disposition of the sequences – grouped into two units (*CPU-1* and *CPU-2*) in the form of an offlap model – is indicative of the progradation of the system and the migration of the coastline towards the sea. This progradation can be followed on the surface by delineating the ridge-and-swale system of the terrain, marked by the positive relief of the ridges. This progradation occurred on an erosive unconformity that cuts on the basal unit (*BU*).

A body of bioturbated grey clay facies (*Fb*) (*CPU-3*) was detected in the most continental zone, beyond the ridges formed by the units described above, but before the ancient palaeocliff. These facies can clearly be interpreted as intertidal flat facies developed in a salt marsh environment, under the protection from the waves by sandy bodies. Similar deposits have been observed in Holocene tidal flats in the surrounding estuaries (Granja et al., 1984; Pendón et al., 1998; Dabrio et al., 2000; Morales-Mateo et al., 2020; Caporizzo et al., 2021). This sedimentary body has been defined as CPU-3, and also appears above the basal unit (*BU*) interdigitated with CPU-1.

5.2. Geodynamic and geomorphological evolution from MIS 5 to the present

The morphologies of the littoral strands on the coastal plain between Chipiona and Sanlúcar de Barrameda are very similar to other Holocene age sandy barriers in the Gulf of Cádiz (Zazo et al., 1994; Dabrio et al., 2000; Rodríguez-Polo et al., 2009; Rodríguez-Ramírez et al., 2016). They usually consist of narrow, elongated accumulative forms arranged subparallel to the coastline, with a clear alternation between ridges and swales (Rovere et al., 2016). In the same way, similar formations of Pleistocene age have been described in the lower coastal plain of Georgia (USA) (Hoyt and Hails, 1967), and the south coast of South Africa (Cawthra et al., 2020), among others. In all cases, these geomorphological structures constitute the record of the past marine dynamics that built a depositional coast associated with a given sea level (Kelsey, 2015). These different depositional units lie on a rocky substratum from the Lower Pleistocene constituted by the basal unit (*BU*: 1.1 Ma) composed of a nearshore-beach sequence found in the present intertidal zone as a shore platform. These same units, of relatively similar age, appear further to the southeast along the Gulf of Cádiz, both in the intertidal zone and along low cliffs parallel to the present coast (Aguirre, 1995; González-Acebrón et al., 2016).

The unconformity between the basal unit (*BU*) and the Late Pleistocene beach ridges encompasses an important hiatus of approximately 1 Ma, during which erosion erased all vestiges of possible intermediate sediments. This phenomenon occurred in large sectors of the Gulf of Cádiz, where the Quaternary neotectonic movements conditioned the distribution of emerged and submerged areas during Pleistocene eustatic highstands (González-Acebrón et al., 2016). In this particular case, it may be hypothesised, during the Lower Pleistocene, coeval with a prolonged lowstand period (Calabrian Stage), the Guadalquivir River flowed around the Chipiona headland to the west and then to the SE, forming an extensive flood plain. This situation could have occurred during MIS 30 or 34. The lateral migration of the river channel around this point would have eroded possible coastal deposits formed in the subsequent eustatic cycles, or would have prevented their development. In any case, the lack of available data precludes greater precision.

During the Middle Pleistocene, a broad coastal plain developed in front of the Chipiona headland (Fig. 11A). In a much later period, at the end of MIS 6, a rapid sea level rise took place in parallel with the beginning of the Eemian interglacial period, sub-stage MIS 5e (Shackleton et al., 2003), which saw significant coastal erosion and cliff development (Fig. 11B). Once the sea level stabilized, the resulting coastal morphology and the orientation of the new shoreline conditioned the onset of a local littoral drift contrary to the regional one, that is, a locally prevailing coastal current directed to the North (Fig. 11C).

The entire set of ridges and swales exhibits the morphology of a littoral sandy barrier system that, probably due to the local drift flowing to the north (Fig. 11C), started growing from the southern side of the river mouth. From that moment onwards, the successive ridges prograded as the result of an offlap mechanism, whereby the littoral strands slightly lost elevation (Fig. 11C). To the north, the palaeo-Guadalquivir developed a system of sandy barriers and dunes on its right bank.

To the east, between the littoral strands and the Mio-Pliocene relief, CPU-3 would correspond to the tidal flats associated with a small estuary or lagoon located in the leeward, sheltered area of the littoral barrier

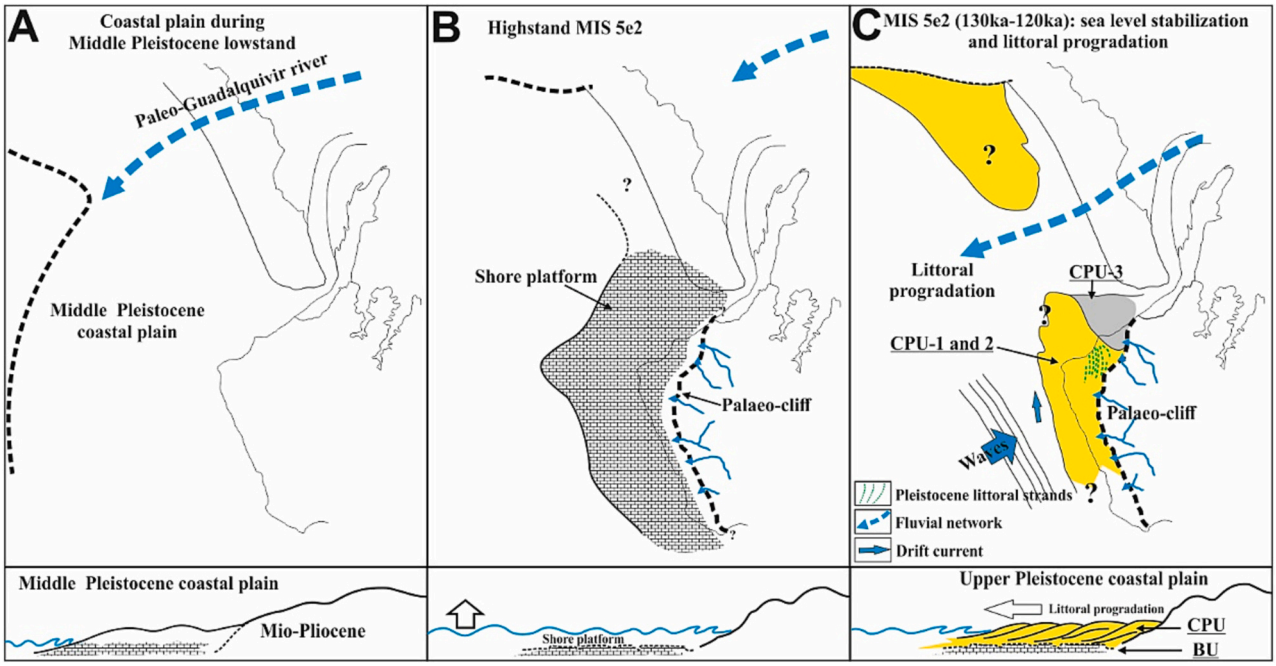

Fig. 11. Palaeogeographical reconstruction of the initial stages of development of the Pleistocene deposits around the mouth of the Guadalquivir River. A: Coastal plain during Middle Pleistocene lowstand. B.- Palaeocliff during the highstand MIS 5e and shore platform genesis (Basal unit: *BU*). C.- Sea level stabilization during MIS 5e and 5c and coastal progradation (Coastal plain units: *CPU-1*, *2* and *3*).

(shaded grey in Fig. 11C). The sandy interdigitations between CPU-3 and the remains of highly transported malacofauna would correspond to washover fans produced during storms that would have affected the old barrier of CPU-1. This is a facies model very similar to those present today in some Holocene littoral spits on the Gulf of Cádiz (Morales et al., 2006; Dabrio et al., 2000; Rodríguez-Ramírez et al., 2019; Gracia et al., 2022).

The numerous interspersed gravel levels, especially in CPU-2, could be related to an increased frequency of storms. According to Zazo et al. (2003), coarse textures during MIS 5e in the Balearic Islands suggest more humid climate conditions and increased frequency of storms in the Western Mediterranean Sea.

The morphosedimentary sequences described in Mallorca suggest the existence of three highstands during MIS 5e (Fig. 12), from 135 to 117 ka (Hillaire-Marcel et al., 1996; Zazo et al., 2013), although in the Canary Islands, only two of these three highstands are usually preserved (Zazo et al., 2003). The second (~130–120 kyr) is considered the most stable highstand worldwide (Bardají et al., 2009). Taking into account the range of dates obtained (150–104 ka) from the end of MIS 6 to MIS 5c, it is very likely that the sequences represented by the prograding units CPU-1 and CPU-2 correspond to the highstand MIS 5e, as these are the most prominent forms of the coastal plain (Fig. 11C). The good geomorphological preservation of the littoral strands suggests that these are probably the sedimentary units associated with the highest sea levels recorded in the Gulf of Cádiz during the last interglacial: the second highstand 5e (~130–120 kyr).

According to the topographic elevation of these units, this relative sea level would have been about 7–8 m above the current mean sea level in the Gulf of Cádiz. Kopp et al. (2009) and Dutton and Lambeck (2012) estimated a global sea level rise of about +6–9 m above the present level for the Eemian episode. Stratigraphic records from the Mediterranean Spanish coasts establish a eustatic episode reaching a maximum range of 7–8 m in the MIS 5e (Zazo et al., 2013), or 2–10 m according to Stocchi et al. (2018), which would be in line with the values established in the study area.

After the transgressive maximum of MIS 5e, a gradual drop in sea level and a progressive continentalization of the area took place. These formations were affected by karst processes and the later generation of a laminar calcrete. It would be at this point that the sedimentary RSU began to be deposited, in correspondence with MIS 5b. This could be interpreted as related to alluvial deposits from surface runoff that drained the surrounding reliefs towards the sea (Fig. 13A). This type of calcrete, associated with lowstands, is widespread, covering different Pleistocene coastal deposits in the region. In the nearby Bay of Cádiz, Gracia et al. (2008) described a similar edaphic carbonate layer covering a Pleistocene beach level dated to 31 ka BP (MIS 3). The calcrete was dated to 19.9–21.7 ka BP (the lowstand associated with the last glacial maximum).

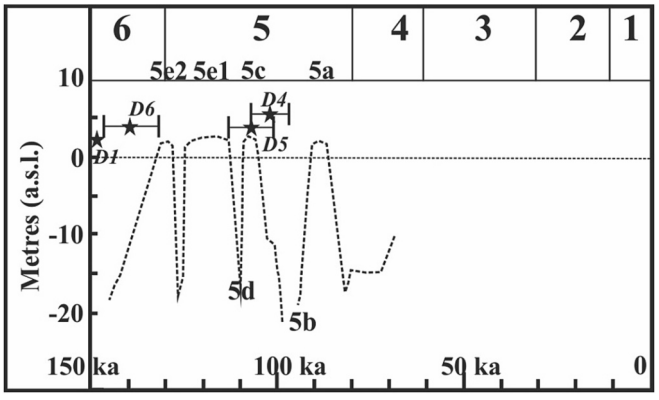

Fig. 12. Eustatic curve of the last interglacial period in Mallorca, Western Mediterranean (Tuccimei et al., 2000) and dated samples from the coastal plain and red sands units at Chipiona. (For interpretation of the references to color in this figure legend, the reader is referred to the web version of this article.)

Currently, a large number of alluvial fans can be observed covering the eastern margin of the Pleistocene coastal plain (Fig. 13B). A drop in sea level after MIS 5e caused an incision of the fluvial network on the Pleistocene deposits and their partial erosion in this sector. The RSU represents the sedimentary filling in of the erosive incision up to the current interglacial, mainly covering the Pleistocene units. The rise in sea level during the Holocene shaped the current coastline and favored the gradual erosion of the Late Pleistocene formations.

According to Pedoja et al. (2011) and Rovere et al. (2016), tectonic processes may have altered the evidence of past sea levels from fossil shoreline records worldwide. In this regard, the location of the study area in the proximity of the westernmost convergent limit between the European and African plates, an area with active tectonics (González-Castillo et al., 2015; Pérez-Peña et al., 2020) (Fig. 1), should be taken into account. Data from the western Betic Cordillera indicate a very consistent westward motion with respect to the relatively stable Iberian Massif foreland (Ruiz-Constán et al., 2012; González-Castillo et al., 2015). The westernmost sector of the Cordillera is undergoing compression, concentrated on a deformation band affected mainly by folds and reverse fault systems, and active at least since the Late Miocene.

The study zone is located to the west of this active band, and was traditionally considered an inactive thrust. However, according to González-Castillo et al. (2015), the mountain front that forms the palaeocliff in Chipiona is tectonically active, and the tectonic compression would be accommodated by active folds. Here, both the Pleistocene plain under study and the old Pleistocene cliff are conditioned by two families of faults running SW-NE and SSE-NNW (IGME, 1998) (Fig. 1), with respect to the highest Mio-Pliocene outcrops beyond the palaeocliff. At a regional scale, the southern Portuguese coast (Figueiredo et al., 2013), the active southern and SW margins of the Betic Orogene (Bardají et al., 2009) and the Strait of Gibraltar (Rodríguez Vidal and Cáceres, 2005; El-Abdellaoui et al., 2016) are characterized by tectonic uplift. The coastal sector of the Gulf of Cádiz (former Guadalquivir foreland basin) was mainly sinking during the Pleistocene (González-Castillo et al., 2015), but during the Late Pleistocene it experienced vertical movements with differentiated areas of downthrown and raised blocks (Zazo et al., 2003; Silva et al., 2006; Pérez-Peña et al., 2020).

However, there is an evident equivalence between the Basal Unit of Chipiona and the Pleistocene deposits in the Bay of Cádiz, as described and dated by González-Acebrón et al. (2016). At 20 km apart, both deposits lie at exactly the same height with respect to the present sea level. The rather low seismicity (Stich et al., 2020) and the scarcity of faults affecting Quaternary deposits in this zone and its proximal surroundings (Gracia et al., 2008) lead us to consider that neotectonic activity here is very low. So, despite the vertical tectonic movements recorded in the Strait of Gibraltar and western Betics during the Pliocene and Early Pleistocene (Rodríguez-Vidal et al., 2004), according to the data presented in this work, the study area can be considered relatively stable in the last stages of the Pleistocene. The level of the deposits could therefore be considered as a reasonable representation of the eustatic level during MIS 5e. The virtual repetition of heights attained by the last two eustatic maximum periods, MIS 5e and the present, is crucial for understanding the climatic components of the present and future evolution of sea level (Waelbroeck et al., 2002; Grant et al., 2012).

Finally, due to their scarcity, Pleistocene coastal deposits like those described in the present work should be preserved and managed as valuable geological heritage, worth being made known publically and divulgated. Heritage protection measures are mainly required for elements located on the coast, where erosion and wave action can episodically damage them (Fernández-Montblanc et al., 2022). In this respect, Spanish Law 42/2007 (Natural Heritage and Biodiversity) includes the concepts of geodiversity and geological heritage, and

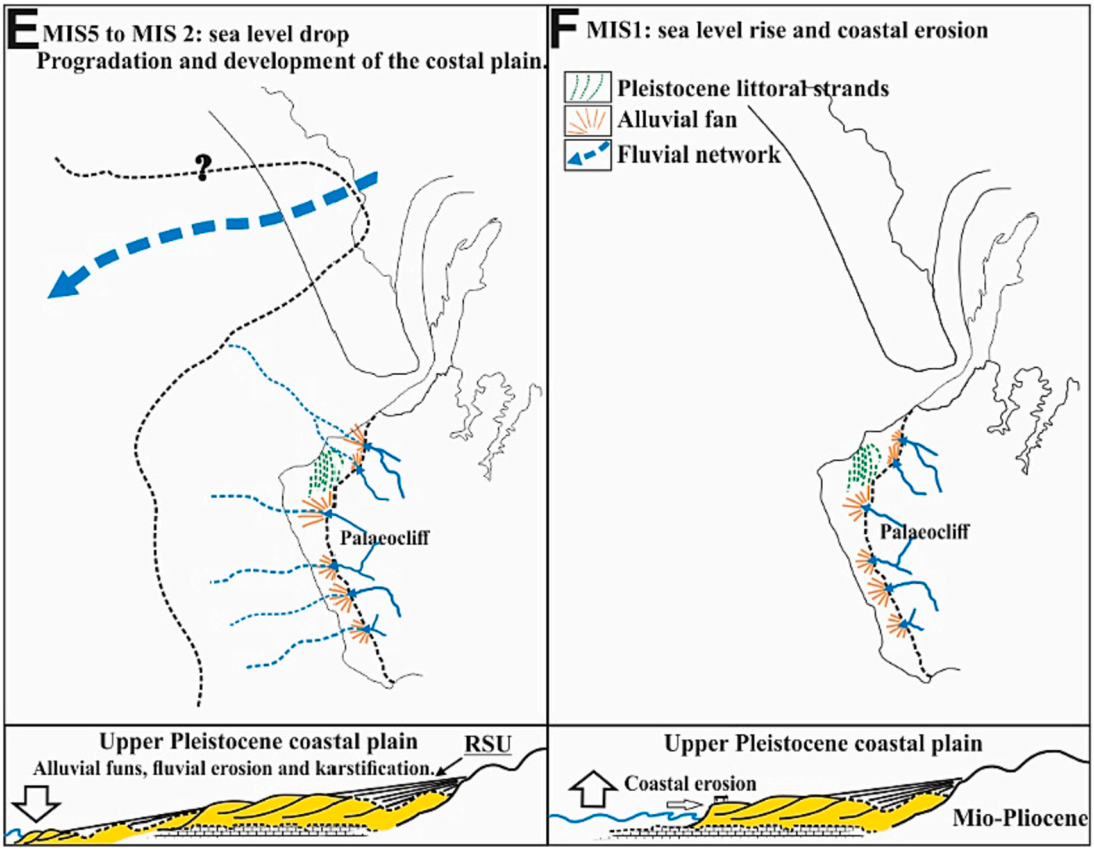

Fig. 13. Palaeogeographical reconstruction of the morphological evolution of the coastal sedimentary plain to the south of the mouth of the Guadalquivir River during the Upper Pleistocene and Holocene. A.- Maximum lowstand reached by the end of the last glacial period and development of a divergent fluvial network. B.- Holocene eustatic transgression and flooding of the previous coastal plain until the present coastal outline was reached.

prescribes geoconservation and sustainable use of these resources under the auspices of regional administrations. These principles were applied by Costa-Casais and Caetano (2013) to several Pleistocene coastal deposits in NW Spain. According to the Spanish Geological Survey (IGME, 1998; García-Cortés et al., 2000), the SW coast of Spain constitutes a geomorphological framework of international interest for a variety of reasons, including the varied Quaternary geoarchives recognized along the shore (Gracia, 2008). The present contribution should be incorporated into that framework and protected accordingly.

6. Conclusions

The analysis of geomorphological and sedimentological patterns, with the support of a high-resolution altimetric study (LiDAR), and the establishment of a chronological context by $^{87}Sr/^{86}Sr$ and OSL dating, has allowed to reconstruct the palaeogeographical, environmental and eustatic evolution of an extensive Quaternary coastal plain in the central area of the Gulf of Cádiz, on the left bank of the mouth of the Guadalquivir River. The Quaternary coastal plain was characterized by a series of ridges and swales, in the form of littoral strands on a littoral barrier, with a sheltered lagoon or salt marsh behind. In this case, the maximum elevation of the Pleistocene deposits reaches about 8 m above mean sea level, and are limited by a paleo-cliff to the east, where Mio-Pliocene formations extend.

In the intertidal zone there is a shore platform associated with a stratigraphic unit (Basal unit, *BU*), which constitutes the substrate, or basement, of the coastal plain. The unit is a scarcely visible unconformity, dated to ca. 1.1 Ma BP, and constituted by a sequence of facies composed of alternating fine sandstones (*Sh*), very coarse sandstone (*Sp*) and conglomerate facies (*Gp*), corresponding to a nearshore-beach sequence. Three stratigraphic units are defined on the coastal plain, with a sedimentary sequence of facies. The first two of these units are comprised of a lower unit (*CPU-1*) and an upper unit (*CPU-2*). This latter is constituted by a fining-upward sequence of conglomerate facies (*G*), from a pebble beach foreshore; crossbedded sands (*St*) typical of a foreshore environment with bar attachment; parallel laminated silty sands (*SFl*) characteristic of a dissipative beach; and ending with root-bioturbated silty sands (*SFb*), corresponding to supratidal/aeolian backshore environments. A third unit (*CPU-3*), constituted by dense greenish-grey clay facies (*Fb*), interdigitates with the sandy facies of CPU-1. This unit has been interpreted as a small salt marsh linked to an estuary or lagoon located in the leeward of the littoral barrier. The disposition of the sequence of the CPU is indicative of the progradation of a littoral barrier system and the migration of the coastline towards the sea.

The deposition of CPU-1 and CPU-2 units dates from from the end of MIS 6 to MIS 5c, but if we consider that the MIS 5e2 (~130–120 kyr) is considered to be the most stable highstand worldwide, this sequence very likely corresponds to this highstand. At the top of all the sequences in the CPUs is an erosive unconformity of karstic origin, on which sit the red silty sand facies (SFm) of the red sands unit (*RSU*). These facies, covering most of the Pleistocene coastal units, could be interpreted as related to alluvial deposits. These would indicate a gradual drop in sea level to the current interglaciar height, and a progressive continentalization of the area, affected by karst processes. Regionally, these karstic processes are associated with the last glacial maximum.

According to the topographic elevation of these CPU units, and the regional correlation with similar formations in the Mediterranean Spanish coasts, the relative sea level would be about 7–8 m above the current mean sea level in the Gulf of Cádiz. From a tectonic point of

view, the study area can be considered as relatively stable in the latter stages of the Pleistocene, and the level of the deposits could thus be regarded as a reasonable representation of the eustatic level during MIS 5e. Consequently, it could represent a valid estimation of the possible rise in sea level in the present interglacial.

Coastal geoarchives like the ones described and analyzed in the present work should be preserved and managed as valuable geological heritage.These help researchers envisage a more realistic picture of the rates and trends of sea level change during the Late Quaternary, and the lateral extent of the effects exerted by tectonics linked to alpine orogens.

CRediT authorship contribution statement

Antonio Rodríguez-Ramírez: Investigation, Writing – original draft, Writing – review & editing. **Francisco Javier Gracia:** Investigation, Writing – original draft, Writing – review & editing. **Juan Antonio Morales:** Investigation. **Diego García:** Investigation. **Eduardo Mayoral:** Investigation.

Declaration of competing interest

The authors declare that they have no known competing financial interests or personal relationships that could have appeared to influence the work reported in this paper.

Data availability

Data will be made available on request.

Acknowledgements

The investigation has been made possible by the financial support of the Regional Government of Andalusia (Junta de Andalucía) to Research Groups RNM276, RNM328, and of the Science & Technology Centre (Centro Científico-Tecnológico) of Huelva to the Department of Applied Geoscience. The present paper contributes to Project IGCP 725, Forecasting coastal change. Funding for open access charge: Universidad de Huelva / CBUA.

References

Achab, M., Moral Cardona, J.P., Gutiérrez-Mas, J.M., Sánchez Bellón, A., González-Caballero, J.L., 2017. Sedimentary provenance and depositional history of Cádiz Bay (SW Spain) based on the study of heavy minerals surface textures. Thalassas 33, 29–42. Available at. https://doi.org/10.1007/s41208-016-0018-6.

Aguirre, J., 1995. Implicaciones paleoambientales y paleogeográficas de dos discontinuidades paleogeográficas en dos depósitos pliocénicos de Cádiz (SW de España). Rev. Soc. Geol. Esp. 8, 161–174 (In Spanish). Available at. https://sge.usal.es/archivos/REV/8(3)/Art04.pdf.

Bardají, T., Goy, J.L., Zazo, C., Hiltaire-Marcel, C., Dabrio, C.J., Cabelo, A., Ghaleb, B., Silva, P.G., Lario, J., 2009. Sea-level and climate changes during OIS 5 in western Mediterranean (Spain). Geomorphology 104, 22–37. Available at. https://doi.org/10.1016/j.geomorph.2008.05.027.

Bateman, M.D., Holmes, P.J., Carr, A.S., Horton, B.P., Jaiswal, M.K., 2004. Aeolianite and barrier dune construction spanning the last two glacial-interglacial cycles from the southern Cape coast, South Africa. Quat. Sci. Rev. 23, 1681–1698. Available at. https://doi.org/10.1016/j.quascirev.2004.02.001.

Benavente, J., Gracia, F.J., López-Aguayo, F., 2000. Empirical model of morphodynamic beachface behaviour for low-energy mesotidal environments. Mar. Geol. 167, 375–390. Available at. https://doi.org/10.1016/S0025-3227(00)00036-0.

Benedetti, M.M., Haws, J.A., Funk, C.L., Daniels, J.M., Hesp, P.A., Bicho, N.F., Minckley, Ellwood, B.B., Forman, S.L., 2009. Late Pleistocene raised beaches of coastal Estremadura, central Portugal. Quat. Sci. Rev. 28, 3428–3447. Available at. https://doi.org/10.1016/j.quascirev.2009.09.029.

Boak, E.H., Turner, I.L., 2005. Shoreline definition and detection: a review. J. Coast. Res. 21, 688–703. Available from. https://doi.org/10.2112/03-0071.1.

Borrego, J., Ruiz, F., González-Regalado, M.L., Pendón, J.G., Morales, J.A., 1999. The Holocene transgression into the estuarine central basin of the Odiel River mouth (Cadiz gulf, SW Spain): lithology and faunal assemblages. Quat. Sci. Rev. 18, 769–788. Available at. https://doi.org/10.1016/S0277-3791(97)00085-1.

Boski, T., Camacho, S., Moura, D., Fletcher, W., Wilamowski, A., Veiga-Pire, C., Correia, V., Loureiro, C., Santana, P., 2008. Chronology of the sedimentary processes during the postglacial sea level rise in two estuaries of the Algarve coast, Southern Portugal. Estuar. Coast. Shelf Sci. 77, 230–244. Available at. https://doi.org/10.1016/j.ecss.2007.09.012.

Caporizzo, C., Gracia, F.J., Aucelli, P.P.C., Barbero, L., Martín-Puertas, C., Lagóstena, L., Ruiz, J.A., Alonso, C., Mattei, G., Galán-Ruffoni, I., López-Ramírez, J.A., Higueras-Milena, A., 2021. Late-Holocene evolution of the Northern Bay of Cádiz from geomorphological, stratigraphic and archaeological data. Quat. Int. 602, 92–109. Available at. https://doi.org/10.1016/j.quaint.2021.03.028.

Cawthra, H.C., Anderson, R.J., De Vynck, J.C., Jacobs, Z., Jerardino, A., Kyriacou, K., Marean, C., 2020. Migration of Pleistocene shorelines across the Palaeo-Agulhas Plain: evidence from dated sub-bottom profiles and archaeological shellfish assemblages. Quat. Sci. Rev. 235, 106107. Available at. https://doi.org/10.1016/j.quascirev.2019.106107.

Chappell, J., Omura, A., Esat, T., McCulloch, M., Pandolfi, J., Ota, Y., Pillans, B., 1996. Reconciliation of late Quaternary sea levels derived from coral terraces at Huon Peninsula with deep sea oxygen isotope records. Earth Planet. Sci. Lett. 141, 227–236. Available at. https://doi.org/10.5026/jgeography.104.5_777.

Clifton, H.E., 1969. Beach lamination: nature and origin. Mar. Geol. 7, 553–559. Available at. https://doi.org/10.1016/0025-3227(69)90023-1.

Clifton, H.E., 1976. Wave-formed sedimentary structures-a conceptual model. In: Davis, R.A., Ethington, R.L. (Eds.), Beach and Nearshore Processes. SOC. Econ. Paleontol. Mineral., Spec. Publ. 24, 126–148. https://doi.org/10.2110/pec.76.24.0126. Available at.

Clifton, H.E., 2006. A Reexamination of Facies Models for Clastic Shorelines. Society for Sedimentary Geology, Special Publication, 84, pp. 293–338.

Costa-Casais, M., Caetano, M.I., 2013. Geological Heritage at risk in NW Spain. Quaternary Deposits and landforms of "Southern Coast" (Baiona-A Garda). Geoheritage 5, 227–248. Available at. https://doi.org/10.1007/s12371-013-0083-7.

Cracknell, A.P., 1999. Remote sensing techniques in estuaries and coastal zones – an update. Int. J. Remote Sens. 19, 485–496. Available at. https://doi.org/10.1080/014311699213280.

Dabrio, C.J., Zazo, C., Goy, J.L., Sierro, J., Borja, F., Lario, J., Gonzalez, J.A., Flores, J.A., 2000. Depositional history of estuarine infill during the last postglacial transgression (Gulf of Cadiz, Southern Spain). Mar. Geol. 162, 381–404. Available at. https://doi.org/10.1016/S0025-3227(99)00069-9.

Dashtgard, S.E., Gingras, M.K., 2005. The temporal significance and distribution of bioturbation in coarse-grained upper foreshore and backshore deposits: waterside Beach, New Brunswick, Canada. Palaios 20, 589–595. Available at. https://doi.org/10.2110/palo.2003.p03-118.

Davidson-Arnott, R.G.D., Greenwood, B., 1974. Bedforms and structures associated with bar topography in the shallow-water wave environment. J. Sediment. Petrol. 44, 698–704. Available at. https://doi.org/10.1306/74D72AE0-2B21-11D7-8648000102C1865D.

Delgado, J., Boski, T., Nieto, J.M., Pereira, L., Moura, D., Gomes, A., Sousa, C., García-Tenorio, R., 2012. Sea-level rise and anthropogenic activities recorded in the late Pleistocene/Holocene sedimentary infill of the Guadiana Estuary (SW Iberia). Quat. Sci. Rev. 33, 121–141. Available at: https://doi.org/10.1016/j.quascirev.2011.12.002.

Domínguez, L., Anfuso, G., Gracia, F.J., 2005. Vulnerability assessment of a retreating coast in SW Spain. Environ. Geol. 47, 1037–1044. Available at. https://doi.org/10.1007/s00254-005-1235-0.

Durcan, J., King, G., Duller, G.A.T., 2015. DRAC: Dose Rate and Age Calculator for trapped charge dating. Quat. Geochronol. 28, 54–61. Available at. https://doi.org/10.1016/j.quageo.2015.03.012.

Dutton, A., Lambeck, K., 2012. Ice volume and sea level during the last interglacial. Science 337, 216–219. Available at. https://doi.org/10.1126/science.1205749.

El-Abdellaoui, J.E., Petit, F., Ghaleb, B., Ozer, A., 2016. Sea-level fluctuation during MIS 5e and geomorphological context on the southern coast of the Strait of Gibraltar (Morocco). Geomorphol. Relief Processus Environ. 22 (3), 287–301. Available at. https://doi.org/10.4000/geomorphologie.11467.

Fairbanks, R.G., Mortlock, R.A., Chiu, T.C., Cao, L., Kaplan, A., Guilderson, T.P., Fairbanks, T.W., Bloom, A.L., Grootes, P.M., Nadeau, M.J., 2005. Radiocarbon calibration curve spanning 0 to 50,000 years BP based on paired 230Th/234U/238U and 14C dates on pristine corals. Quat. Sci. Rev. 24, 1781–1796. Available at. https://doi.org/10.1016/j.quascirev.2005.04.007.

Farrell, J.W., Clemens, S.C., Gromet, L.P., 1995. Improved chronostratigraphic reference curve of late Neogene seawater 87Sr/86Sr. Geology 23, 403–406 (Available at doi: 10.1130/0091-7613(1995)023<0403:ICRCOL>2.3.CO;2).

Fernández-Montblanc, T., Bethencourt, M., Izquierdo, A., 2022. Underwater cultural heritage risk assessment methodology for wave-induced hazards: the showcase of the Bay of Cadiz. Front. Mar. Sci. 9, 1005514. Available at. https://doi.org/10.3389/fmars.2022.1005514.

Figueiredo, P.M., Cabral, J., Rockwell, T.K., 2013. Recognition of Pleistocene marine terraces in the Southwest of Portugal (Iberian Peninsula): evidences of regional Quaternary uplift. Ann. Geophys. 56 (n.6) https://doi.org/10.4401/ag-6276. Special Issue Earthquake Geology. Available at.

Galbraith, R.F., Roberts, R.G., Laslett, G.M., Yoshida, H., Olley, J.M., 1999. Optical dating of single and multiple grains of quartz from Jinmium rock shelter, northern Australia: part I, experimental design and statistical models. Archaeometry 41, 339–364. Available at. https://doi.org/10.1111/j.1475-4754.1999.tb00987.x.

García-Cortés, A., Barettino, D., Gallego, E., 2000. Inventory and Cataloguing of Spain's Geological Heritage. A Historical Review and Proposals for the Future. In: Geological Heritage: Its Conservation and Management (Barettino, D., Wimbledon, W.A.P., Gallego, E., Eds.). IUGS, Madrid, p. 47.67.

García-Moreno, D., Gupta, S., Collier, J.S., Oggioni, F., Vanneste, K., Trentesaux, A., Verbeeck, K., Versteeg, W., Jomard, H., Camelbeeck, Th., De Batist, M., 2019. Middle–Late Pleistocene landscape evolution of the Dover Strait inferred from buried

and submerged erosional landforms. Quat. Sci. Rev. 203, 209–232. Available at. https://doi.org/10.1016/j.quascirev.2018.11.011.
García-Novo, F., Marín Cabrera, C., 2006. Doñana: Water and Biosphere, Doñana 2005 Project. Guadalquivir Hydrologic Basin Authority, Spanish Ministry of the Environment, Madrid.
González-Acebrón, L., Mas, R., Arribas, J., Gutiérrez-Mas, J.M., Pérez-Garrido, C., 2016. Very coarse-grained beaches as a response to generalized sea level drops in a complex active tectonic setting: Pleistocene marine terraces at the Cadiz coast, SW Spain. Mar. Geol. 382, 92–110. Available at. https://doi.org/10.1016/j.margeo.2016.09.007.
González-Castillo, L., Galindo-Zaldívar, J., de Lacy, M.C., Borque, M.J., Martínez-Moreno, F.J., García-Armenteros, Gil, A.J., 2015. Active rollback in the Gibraltar Arc: Evidences from CGPS data in the western Betic Cordillera. Tectonophysics 663, 310–321. Available at. https://doi.org/10.1016/j.tecto.2015.03.010.
Goy, J.L., Zazo, C., Dabrio, C., Lario, J., Borja, F., Sierro, F.J., Flores, J.A., 1996. Global and regional factors controlling changes of coastlines in Southern Iberia (Spain) during the Holocene. Quat. Sci. Rev. 15, 773–780. Available at. https://doi.org/10.1016/S0277-3791(96)00071-6.
Gracia, F.J., 2008. Costas bajas de la Península Ibérica. In: García-Cortés, A., Agueda, J., Palacio, J., Salvador, C.I. (Eds.), Spanish Geological Frameworks and Geosites. Contextos geológicos españoles. Una aproximación al patrimonio geológico español de relevancia internacional, Instituto Geológico y Minero de España, Madrid, pp. 192–199 (In Spanish).
Gracia, F.J., Rodríguez-Vidal, J., Belluomini, G., Cáceres, L.M., Benavente, J., Alonso, C., 2008. Diapiric uplift of an MIS 3 marine deposit in SW Spain. Implications in Late Pleistocene sea level reconstruction and palaeogeography of the Strait of Gibraltar. Quat. Sci. Rev. 27 (23–24), 2219–2231. Available at. https://doi.org/10.1016/j.quascirev.2008.08.013.
Gracia, F.J., Alonso, C., Giles, F., Benavente, J., Del Río, L., 2010. Evidencias del paso del río Guadalquivir por el interior de la Bahía de Cádiz durante el Pleistoceno Medio. In: Cuaternario y Arqueología. Homenaje a Francisco Giles Pacheco. Servicio de Publicaciones, Diputación Provincial de Cádiz, p. 9-17. I.S.B.N.:978-84-96654-49-5 (In Spanish).
Gracia, F.J., Alonso, C., Aparicio, J.A., 2022. The record of energetic marine events in the Bay of Cadiz during historical times. In: Historical Earthquakes, Tsunamis and Archaeology in the Iberian Peninsula (Álvarez, M., Machuca, F., Eds.). Springer, Heidelberg, pp. 151–176. Available at. https://doi.org/10.1007/978-981-19-1979-4_7.
Granja, H., Froidefond, J.-M., Pera, T., 1984. Processus d'evolution morpho-sedimentaire de la Ria Formosa (Portugal). Bull. Inst. Geol. Bassin Aquitaine, Bordeaux 36, 37–50.
Grant, K.M., Rohling, E.J., Bar-Matthews, M., Ayalon, A., Medina-Elizalde, M., Ramsey, C.B., Satow, C., Roberts, A.P., 2012. Rapid coupling between ice volume and polar temperature over the past 150,000 years. Nature 491, 744–747. Available at. https://doi.org/10.1038/nature11593.
Grützner, C., Reicherter, K., Hübscher, C., Silva, P.G., 2012. Active faulting and neotectonics in the Baelo Claudia area, Campo de Gibraltar (southern Spain). Tectonophysics 554-557, 127–142. Available at: https://doi.org/10.1016/j.tecto.2012.05.025.
Guerin, G., Mercier, N., Adamiec, G., 2011. Dose-rate conversion factors: update. Ancient TL 29, 5–8.
Gutiérrez-Mas, J.M., Mas, R., 2013. Record of the high energy events in Plio-Pleistocene marine deposits of the Gulf of Cadiz (SW Spain): facies and processes. Facies 59 (4), 679–701. Available at. https://doi.org/10.1007/s10347-012-0344-y.
Gutiérrez-Mas, J.M., Hernández-Molina, F.J., López-Aguayo, F., 1996. Holocene sedimentary dynamics on the Iberian continental shelf of the Gulf of Cádiz (SW Spain). Cont. Shelf Res. 16 (13) https://doi.org/10.1016/0278-4343(96)00010-6 (1635-165, Available at).
Hernández-Molina, F.J., Somoza, L., Vázquez, J.T., Lobo, F., Fernández-Puga, M.C., Llave, E., Díaz-del Río, V., 2002. Quaternary stratigraphic stacking patterns on the continental shelves of the southern Iberian Peninsula: their relationship with global climate and palaeoceanographic changes. Quat. Int. 92, 5–23. Available at. https://doi.org/10.1016/S1040-6182(01)00111-2.
Hillaire-Marcel, C., Gariepy, C., Ghaleb, B., Goy, J.L., Zazo, C., Cuerda, J., 1996. U-series measurements in Tyrrhenian deposits from Mallorca. Further evidence for two last interglacial high sea-levels in the Balearic Islands. Quat. Sci. Rev. 15, 53–62. Available at. https://doi.org/10.1016/0277-3791(95)00079-8.
Horn, D.P., Walton, S.M., 2007. Spatial and temporal variations of sediment size on a mixed sand and gravel beach. Sediment. Geol. 202, 509–528. Available at. https://doi.org/10.1016/j.sedgeo.2007.03.023.
Hoyt, J.H., Hails, J., 1967. Pleistocene shoreline sediments in Coastal Georgia: deposition and modification. Science 155, 1541–1543. Available at. https://doi.org/10.1126/science.155.3769.1541.
IGME, 1998. Mapa Neotectónico de España 1:1.000.000, Servicio de Publicaciones del Ministerio de Industria. Madrid.
Inman, D.L., Nordstrom, C.E., 1971. On the tectonic and morphologic classification of coasts. J. Geol. 79, 1–21. Available at. https://doi.org/10.1086/627583.
Kelsey, H.M., 2015. Geomorphological indicators of past sea levels. In: Handbook of Sea-Level Research (Shennan, I., Long, A.J., Horton, B.P., Eds.). John Wiley & Sons, pp. 66–82. Available at. https://doi.org/10.1002/9781118452547.ch5.
Kirk, R.M., 1980. Mixed sand and gravel beaches: morphology, processes and sediments. Prog. Phys. Geogr. 4, 189–210. Available at. https://doi.org/10.1177/030913338000400.
Kopp, R.E., Simons, F.J., Mitrovica, J.X., Maloof, A.C., Oppenheimer, M., 2009. Probabilistic assessment of sea level during the last interglacial stage. Nature 462, 863–867. Available at. https://doi.org/10.1038/nature08686.
Lario, J., Zazo, C., Dabrio, C.J., Somoza, L., Goy, J.L., Bardají, T., Silva, P.G., 1995. Record of recent Holocene sediment input on spit bars and deltas of South Spain. J. Coast. Res. 17, 241–245.
Lario, J., Spencer, C., Zazo, C., Goy, J.L., Cabero, A., Dabrio, C.J., Bardají, T., Borja, F., Civis, J., Borja, C., Alonso-Azcárate, J., 2015. Evolución del estuario del río Piedras (Huelva) durante el Holoceno. In: Galve, J.P., Azañón, J.M., Pérez Peña, J.V., Ruano, P. (Eds.), XIV Reunión Nacional de Cuaternario. Granada, AEQUA, pp. 28–30.
Martínez-Loriente, S., Gràcia, E., Bartolomé, R., Sallarès, V., Connors, C., Perea, H., Lo Iacono, C., Klaeschen, D., Terrinha, P., Dañobeitia, J.J., Zitellini, N., 2013. Active deformation in old oceanic lithosphere and significance for earthquake hazard: Seismic imaging of the Coral Patch Ridge area and neighboring abyssal plains (SW Iberian Margin). Geochem. Geophys. Geosyst. 14, 2206–2231. Available at. https://doi.org/10.1002/ggge.20173.
Mason, T., Coates, T.T., 2001. Sediment transport processes on mixed beaches: a review for shoreline management. J. Coast. Res. 17 (3), 645–657.
Miall, A.D., 1996. The Geology of Fluvial Deposits. Springer, Berlin, Germany.
Morales, J.A., 1997. Evolution and facies architecture of the mesotidal Guadiana River Delta (S.W. Spain-Portugal). Mar. Geol. 138, 127–148. Available at. https://doi.org/10.1016/S0025-3227(97)00009-1.
Morales, J.A., Cantano, M., Rodríguez-Ramírez, A., Martín, R., 2006. Mapping geomorphology and active processes on the Coast of Huelva (SW Spain). J. Coast. Res. 48, 89–99.
Morales-Mateo, R., Borrego, J., Carro, M., Morales, J.A., 2020. Depositional Facies along the Banks of Guadalquivir Estuary (SW Spain). J. Coast. Res. SI 95, 573–577.
Murray, A.S., Wintle, A.G., 2000. Luminescence dating of quartz using an improved single-aliquot regenerative-dose protocol. Radiat. Meas. 32, 57–73. Available at. https://doi.org/10.1016/S1350-4487(99)00253-X.
Murray, A.S., Wintle, A.G., 2003. The single aliquot regenerative dose protocol: potential for improvements in reliability. Radiat. Meas. 37 (4–5), 377–381. Available at. https://doi.org/10.1016/S1350-4487(03)00053-2.
NEEM community members, 2013. Eemian interglacial reconstructed from a Greenland folded ice core. Nature 493, 489–493. Available at. https://doi.org/10.1038/nature11789.
Otvos, E.G., 2005. Numerical chronology of Pleistocene coastal plain and valley development; extensive aggradation during glacial low sea-levels. Quat. Int. 135, 91–113.l. Available at. https://doi.org/10.1016/j.quaint.2004.10.026.
Pedoja, K., Husson, L., Regard, V., Cobbold, P.R., Ostanciaux, E., Johnson, M.E., Kershaw, S., Saillard, M., Martinod, J., Furgerot, L., Weill, P., Delcaillau, B., 2011. Relative sea-level fall since the last interglacial stage: are coasts uplifting worldwide? Earth Sci. Rev. 108, 1–15. Available at. https://doi.org/10.1016/j.earscirev.2011.05.002.
Pedoja, K., Husson, L., Johnson, M.E., Melnick, D., Witt, C., Pochat, S., Nexer, M., Delcaillau, B., Pinegina, T., Poprawski, Y., Authemayou, C., Elliot, M., Regard, V., Garestier, F., 2014. Coastal staircase sequences reflecting sea-level oscillations and tectonic uplift during the Quaternary and Neogene. Earth Sci. Rev. 132, 13–38. Available at. https://doi.org/10.1016/j.earscirev.2014.01.007.
Pendón, J.G., Morales, J.A., Borrego, J., Jiménez, I., Lopez, M., 1998. Evolution of estuarine facies in a tidal channel environment SW Spain: evidence for a change from tide-to wave-domination. Mar. Geol. 147, 43–62. Available at. https://doi.org/10.1016/S0025-3227(98)00006-1.
Pérez-Peña, J.V., Azañón, J.M., Galve, J.P., Jabaloy, A., Bardají, T., Silva, P.G., Lario, J., Zazo, C., Goy, J.L., Dabrio, C.J., Cabero, A., 2020. Active landscape of the Betic Cordillera. In: The Geology of Iberia: A Geodynamic Approach. Vol. 5: Active Processes: Seismicity, active faulting and relief (Azañón, J.M., Cabral, J.M.L.C., Eds.). Springer, pp. 102–115. Available at. https://doi.org/10.1007/978-3-030-10931-8.
Prescott, J.R., Hutton, J.T., 1994. Cosmic ray contributions to dose rates for luminescence and ESR dating: large depths and long term time variations. Radiat. Meas. 23, 497–500. Available at. https://doi.org/10.1016/1350-4487(94)90086-8.
Roberts, T.M., Wang, P., Puleo, J.A., 2013. Storm-driven cyclic beach morphodynamics of a mixed sand and gravel beach along the Mid-Atlantic Coast, USA. Mar. Geol. 346, 403–421. Available at. https://doi.org/10.1016/j.margeo.2013.08.001.
Rodríguez Vidal, J., Cáceres, L.M., 2005. Evidencias morfológicas erosivas de niveles marinos pleistocenos en la costa del Jbel Musa (N. de Marruecos). In: VI Reunión de Cuaternario Ibérico (Rodríguez Vidal, J., Finlayson, C., Giles, F., Eds.), AEQUA. Gibraltar, pp. 48–49.
Rodríguez-Polo, S., Gracia, F.J., Benavente, J., Del Río, L., 2009. Geometry and recent evolution of the Holocene beach ridges of the Valdelagrana littoral spit (Cádiz Bay, SW Spain). J. Coast. Res. SI 56, 20–23.
Rodríguez-Ramírez, A., Yáñez, C.M., 2008. Formation of chenier plain of the Doñana marshland (SW Spain): observations and geomorphic model. Mar. Geol. 254, 187–196. Available at. https://doi.org/10.1016/j.margeo.2008.06.006.
Rodríguez-Ramírez, A., Rodríguez-Vidal, J., Cáceres, L., Clemente, L., Belluomini, G., Manfra, L., Improta, S., De Andrés, J.R., 1996. Recent coastal evolution of Doñana National Park (Southern Spain). Quat. Sci. Rev. 15, 803–809. Available at. https://doi.org/10.1016/S0277-3791(96)00068-6.
Rodríguez-Ramírez, A., Flores-Hurtado, E., Contreras, C., Villarías-Robles, J.J.R., Jiménez-Moreno, G., Pérez-Asensio, J.M., López-Sáez, J.A., Celestino-Pérez, S., Cerrillo-Cuenca, E., León, A., 2014. The role of neo-tectonics in the sedimentary infilling and geomorphological evolution of the Guadalquivir estuary (Gulf of Cádiz, SW Spain) during the Holocene. Geomorphology 219, 126–140. Available at. https://doi.org/10.1016/j.geomorph.2014.05.004.
Rodríguez-Ramírez, A., Pérez-Asensio, J.N., Santos, A., Jiménez-Moreno, G., Villarías-Robles, J.J.R., Mayoral, E., Celestino-Pérez, S., Cerrillo-Cuenca, E., López-Sáez, J.A., Ángel León, Á., Contreras, C., 2015. Atlantic extreme wave events during the last

four millennia in the Guadalquivir estuary, SW Spain. Quat. Res. 83, 24–40. Available at. https://doi.org/10.1016/j.yqres.2014.08.005.
Rodríguez-Ramírez, A., Villarías-Robles, J.J.R., Pérez-Asensio, J.N., Santos, A., Morales, J.A., Celestino-Pérez, S., Leon, A., Santos-Arévalo, F.J., 2016. Geomorphological record of extreme wave events during Roman times in the Guadalquivir estuary (Gulf of Cadiz, SW Spain): an archaeological and paleogeographical approach. Geomorphology 261, 103–118. Available at. https://doi.org/10.1016/j.geomorph.2016.02.030.
Rodríguez-Ramírez, A., Villarías-Robles, J.J.R., Pérez-Asensio, J.N., Celestino Pérez, S., 2019. The Guadalquivir Estuary: spits and marshes. In: The Spanish Coastal Systems (Morales, J.A., Ed.). Springer Nature, pp. 517–541. Available at. https://doi.org/10.1007/978-3-319-93169-2.
Rodríguez-Vidal, J., Cáceres, L.M., Finlayson, J.C., Gracia, F.J., Martínez-Aguirre, A., 2004. Neotectonics and shoreline history of the Rock of Gibraltar, southern Iberia. Quat. Sci. Rev. 23, 017–2029. Available at. https://doi.org/10.1016/j.quascirev.2004.02.008.
Roldán, F.J., Divar, J., Borrero, J.D., Zazo, C., Goy, J.L., 1988. Memoria y mapa geológico de Sanlúcar de Barrameda E. 1:50.000, Hoja 1047. Instituto Geológico y Minero de España, Madrid (35 pp).
Rovere, A., Raymo, M.E., Vacchi, M., Lorscheid, T., Stocchi, P., Gómez-Pujol, L., Harris, D.L., Casella, E., O'Leary, M.J., Hearty, P.J., 2016. The analysis of Last Interglacial (MIS 5e) relative sea-level indicators: Reconstructing sea-level in a warmer world. Earth Sci. Rev. 159, 404–427. Available at. https://doi.org/10.1016/j.earscirev.2016.06.006.
Ruiz-Constán, A., Pedrera, A., Galindo-Zaldívar, J., Stich, D., Morales, J., 2012. Recent and active tectonics in the western part of the Betic Cordillera. J. Iber. Geol. 38, 161–174. Available at. https://doi.org/10.5209/rev_JIGE.2012.v38.n1.39211.
Sampath, D.M.R., Boski, T., Loureiro, C., Sousa, C., 2015. Modelling of estuarine response to sea-level rise during the Holocene: application to the Guadiana Estuary-SW Iberia. Geomorphology 232, 47–64. Available at. https://doi.org/10.1016/j.geomorph.2014.12.037.
Sanz de Galdeano, C., López Garrido, A.C., 1991. Tectonic evolution of the Málaga Basin (Betic Cordillera). Regional implications. Geodin. Acta 5, 173–186. Available at. https://doi.org/10.1080/09853111.1992.11105226.
Schumm, S.A., 1985. Patterns of alluvial rivers. Annu. Rev. Earth Planet. Sci. 13, 5–27.
Shackleton, N.M., Sánchez-Goñi, M.F., Pailler, D., Lancelot, Y., 2003. Marine Isotope Substage 5e and the Eemian Interglacial. Glob. Planet. Chang. 36, 151–155. Available at. https://doi.org/10.1016/S0921-8181(02)00181-9.
Shepard, F.P., 1954. Nomenclature based on sand–silt–clay ratios. J. Sediment. Res. 24, 151–158. Available at. https://doi.org/10.1306/D4269774-2B26-11D7-8648000102C1865D.
Siddall, M., Rohling, E.J., Thompson, W.G., Waelbroeck, C., 2008. Marine Isotope Stage 3 sea level fluctuations: data synthesis and new outlook. Rev. Geophys. 46, RG4003. Available at. https://doi.org/10.1029/2007RG000226.
Silva, P.G., Goy, J.L., Zazo, C., Bardají, T., Lario, J., Somoza, L., Luque, L., González-Hernández, F.M., 2006. Neotectonic fault mapping at the Gibraltar Strait Tunnel area, Bolonia Bay (South Spain). Eng. Geol. 84, 31–47. Available at. https://doi.org/10.1016/j.enggeo.2005.10.007.
Spanish Ministry of Fomento, 2005. Información climática de nivel del mar. Mareógrafo de Sevilla, Bonanza, Madrid (in Spanish).
Stich, D., Martínez-Solares, J.M., Custodio, S., Batlló, J., Martín, R., Teves-Costa, P., Morales, J., 2020. Seismicity of the Iberian Peninsula. In: The Geology of Iberia: A Geodynamic Approach. Vol. 5: Active Processes: Seismicity, Active Faulting and Relief (Azañón, J.M., Cabral, J.M.L.C., Eds.). Springer, pp. 11–32. Available at. https://doi.org/10.1007/978-3-030-10931-8.
Stocchi, P., Vacchi, M., Lorscheid, T., De Boer, B., Simms, A.R., Van del Wal, R.S.W., Vermeersen, B.L.A., Pappalardo, M., Rovere, A., 2018. MIS 5e relative sea-level changes in the Mediterranean Sea: contribution of isostatic disequilibrium. Quat. Sci. Rev. 185, 122–134. Available at. https://doi.org/10.1016/j.quascirev.2018.01.004.
Tamura, T., 2012. Beach ridges and prograded beach deposits as palaeoenvironment records. Earth Sci. Rev. 114 (3), 279–297. Available at. https://doi.org/10.1016/j.earscirev.2012.06.004.
Tuccimei, P., Ginés, J., Delitala, C., Pazzelli, L., Taddeucci, A., Clamor, B., Fornós, J.J., Ginés, A., Gràcia, F., 2000. Dataciones Th/U de espeleotemas freáticos recolectados a cotas inferiores al actual nivel marino en cuevas costeras de Mallorca (España): aportaciones a la construcción de una curva eustática detallada de los últimos 300 ka para el Mediterráneo occidental. Endins 23, 59–71 (in Spanish).
Vanney, J.-R., 1970. L'hydrologie du bas Guadalquivir. In: Instituto de Geografía Aplicada, C.S.I.C. Madrid (175 p., in French).
Viguier, C., 1977. Les grands traits de la tectonique du basin néogène du Bas Guadalquivir. Bol. Geol. Min. 88, 39–44. Available at. http://geoprodig.cnrs.fr/items/show/123983.
Villwock, J.A., 1984. Geology of the coastal province of Rio Grande do Sul, Southern Brazil. A Synthesis. Pesqui. em Geociênc. 16, 5–49. Available at. 10.22456/1807-9806.21711.
Waelbroeck, C., Labeyric, L., Michel, E., Duplessy, J.C., McManus, J.F., Lambeck, K., Balbon, E., Labracherie, M., 2002. Sea-level and deep water temperature changes derived from benthic foraminifera isotopic records. Quat. Sci. Rev. 21, 295–305. Available at. https://doi.org/10.1016/S0277-3791(01)00101-9.
Whittington, G., Hall, A.M., 2002. The Tolsta Interstadial, Scotland: correlation with D–O cycles GI-8 to GI-5? Quat. Sci. Rev. 21, 901–915. Available at. https://doi.org/10.1016/S0277-3791(01)00068-3.
Wintle, A.G., 1997. Luminescence dating: laboratory procedures and protocols. Radiat. Meas. 27, 769–817. Available at. https://doi.org/10.1016/S1350-4487(97)00220-5.
Zazo, C., 1980. El Cuaternario marino-continental y el límite Plio- Pleistoceno en el litoral de Cádiz. PhD Thesis. Universidad Complutense de Madrid (in Spanish).
Zazo, C., Goy, J.L., Dabrio, C.J., Civis, J., Baena, J., 1985. Paleogeografía de la desembocadura del Guadalquivir al comienzo del Cuaternario (provincia de Cádiz, España). I Reunión del Cuaternario Ibérico, GETC – CTPEQ, Lisboa, vol. 1, pp. 461–472 (in Spanish).
Zazo, C., Goy, J.L., Somoza, L., Dabrio, C.J., Belluomini, G., Improta, S., et al., 1994. Holocene sequence of relative sea level highstand–lowstand in relation to the climatic trends in the Atlantic-Mediterranean linkage coast: Forecast for future coastal changes and hazards. J. Coast. Res. 10 (4), 933–945.
Zazo, C., Silva, P.G., Goy, J.L., Hillaire-Marcel, C., Ghaleb, B., Lario, J., Bardají, T., González, A., 1999. Coastal uplift in continental collision plate boundaries: data from the Last Interglacial marine terraces of the Gibraltar Strait area (South Spain). Tectonophysics 301, 95–109. Available at. https://doi.org/10.1016/S0040-1951(98)00217-0.
Zazo, C., Goy, J.L., Dabrio, C.J., Bardají, T., Hillaire-Marcel, C., Ghaleb, B., Gonzalez-Delgado, J.A., Soler, V., 2003. Pleistocene raised marine terraces of the Spanish Mediterranean and Atlantic coasts: records of coastal uplift, sea-level highstands and climate changes. Mar. Geol. 194, 103–133. Available at. https://doi.org/10.1016/S0025-3227(02)00701-6.
Zazo, C., Mercier, N., Silva, P.G., Dabrio, C.J., Goy, J.L., Roquero, E., et al., 2005. Landscape evolution and geodynamic controls in the Gulf of Cadiz (Huelva Coast, SW Spain) during the Late Quaternary. Geomorphology 68 (3–4), 269–290. Available at. https://doi.org/10.1016/j.geomorph.2004.11.022.
Zazo, C., Dabrio, C.J., Goy, J.L., Lario, J., Cabero, A., Silva, P.G., et al., 2008. The coastal archives of the last 15 ka in the Atlantic-Mediterranean Spanish linkage area: sea level and climate changes. Quat. Int. 181, 72–87. Available at. https://doi.org/10.1016/j.quaint.2007.05.021.
Zazo, C., Goy, J.L., Dabrio, C.J., Lario, J., González-Delgado, J.A., Bardají, T., Hillaire-Marcel, C., Cabero, A., Ghaleb, B., Borja, F., Silva, P.G., Roquero, E., Soler, V., 2013. Retracing the Quaternary history of sea-level changes in the Spanish Mediterranean–Atlantic coasts: geomorphological and sedimentological approach. Geomorphology 196, 36–49. Available at. https://doi.org/10.1016/j.geomorph.2012.10.020.